Universidade da Beira Interior

Faculdade de Ciências da Saúde

Effect of Regucalcin on the expression of oncogenes and tumor suppressor genes in prostate cell lines

Mestrado em Ciências Biomédicas

Cátia Alexandra Vicente Vaz

Covilhã, 2010

Universidade da Beira Interior

Faculdade de Ciências da Saúde

Effect of Regucalcin on the expression of oncogenes and tumor suppressor genes in prostate cell lines

Influência da Regucalcina na expressão de oncogenes e genes supressores de tumor em linhas celulares de próstata

Supervisor: Professora Doutora Sílvia Cristina da Cruz Marques Socorro

Co-supervisor: Professor Doutor Claúdio Jorge Maia Baptista

Mestrado em Ciências Biomédicas

Cátia Alexandra Vicente Vaz

Covilhã, 2010

O conteúdo do presente trabalho é da exclusiva responsabilidade da autora:

_____

Acknowledgements

First and foremost, I would like to thank my supervisor, Profª Drª Sílvia Socorro, for her invaluable support, guidance and friendship.

I would like to thank my co-supervisor for his continuos help and helpful recommendations.

I am grateful to my colleagues and friends Sara Correia, Luis Rato, Inês Gomes, Margarida Gonçalves, Ana Mamede, Vitor Gaspar, Carlos Gaspar and Sandra Laurentino.

I would also like to express my gratitude to our research group and to all present colleagues involved in the Heath sciences research centre of the University of Beira Interior.

I acknowledge Profº Pedro Oliveira and Drª Ana Clara Cristovão for counselling in fluorescence microscopy.

I am also grateful to my family and friends for friendly support during the last year.

Abstract

Regucalcin (RGN) is a calcium-binding protein playing an important role in maintenance of intracellular calcium homeostasis. Because of its diminished expression with aging it is also designated Senescence-marker-protein (SMP30). In addition, RGN suppresses cell proliferation, inhibits expression of oncogenes, and increases the expression of tumor suppressor genes in hepatoma cell lines. Very recently, our research group demonstrated that RGN expression is diminished in prostate cancer tissues, what suggests that RGN may have a protective role against carcinogenesis and, consequently, loss of regucalcin expression may contribute to tumor development. The present project aims to characterize RGN expression in prostate tissues and cell-lines and to determine the role of RGN on the expression of oncogenes and tumour suppressor genes in neopasic and non-neoplasic prostate cells. The expression of RGN in rat prostate at different post-natal ages determined by quantitative PCR analysis showed a significant increase at 3M old rats, maintaining their expression in 6M-old animals and diminishing in the following stages. In this report, we confirmed RGN protein expression in human cancer prostate tissues, and cells lines by Imunohistochemistry and Western Blot, respectively. To analyze the effect of RGN on the expression of oncogenes (BCL2, Ha-ras and c-myc) and tumor supressor genes (p53 and RB1), pIRES/RGN expression vectors were constructed and used to transfect LnCAP, PC3, PNT1A and PNT2 cells. Fluorescence microscopy analysis showed successful transfection of PC3 and PNT1A cells, with RGN-GFP protein localization in cell nuclei and cytoplasm. Analysis of transfection experiments in LnCAP and PNT2 cells, and determination of the effect of RGN on the expression of tumor related genes are underway. Nevertheless, RGN localization in cell nuclei, suggests their likely influence regulating expression of oncogenes and tumor suppressor genes in prostate cell lines overexpressing RGN.

Resumo

A Regucalcina (RGN) é uma proteína de ligação ao cálcio desempenhando um papel importante na homeostase intracelular deste ião. Devido á diminuição da sua expressão associada ao envelhecimento é também designada como Proteína marcadora de senescência (SMP30). A RGN tem sido associada a funções tais como, supressão da proliferação celular, inibição da expressão de oncogenes e aumento na expressão de genes supressores de tumor em linhas celulares de fígado. Recentemente, o nosso grupo de investigação demonstrou que a expressão da RGN estava diminuida em tecidos de adenocarcinomas de próstata, o que sugere um efeito protector da RGN na carcinogénese, e consequentemente a perda da sua expressão pode estar associada ao desenvolvimento tumoral. O presente trabalho teve como objectivos a caracterização da expressão da RGN em linhas celulares e tecidos de próstata e determinar o papel da RGN na expressão de oncogenes e genes supressores de tumor em linhas celulares da próstata neoplásicas e não-neoplásicas. A expressão da RGN na próstata de rato ao longo do desenvolvimento pós-natal foi estudada por PCR quantitativo. A expressão da RGN aumentou aos 3M de idade, a sua expressão manteve-se elevada até aos 6M e diminuiu nas idades seguintes. Neste estudo foi também possível confirmar a expressão da RGN em tecidos de adenocarcinoma de próstata e em linhas celulares por imunohistoquimica e Western Blot, respectivamente. Para analisar o efeito da RGN na expressão de oncogenes e genes supressores de tumor, foram construidos vectores de expressão pIRES/RGN os quais foram usados para transfectar as linhas celulares LnCAP, PC3, PNT1A e PNT2. A análise efectuada por microscopia de fluorescência demonstrou a localização da proteína RGN-GFP no núcleo e citoplama das células PC3 e PNT1A transfectadas com sucesso. A análise da transfecção das celúlas LnCAP e PNT2, bem como a determinação do efeito da RGN na expressão de genes associados ao desenvolvimento tumoral encontra-se em curso. No entanto, os resultados que demonstram a localização da RGN no núcleo, sugerem o seu possível envolvimento na regulação da expressão de oncogenes e genes supressores de tumor em linhas celulares da próstata que sobre-expressam a RGN.

List of Abreviations

Act D	Actinomycin
AR	Androgen receptor
bp	Base pairs
BPH	Benign prostatic hypertrophy
Ca^{2+}	Calcium
CaM kinase	Ca^{2+}/calmodulin-dependent protein kinase
CaR	calcium polyvalent cation-sensing receptor
CCE	Capacitative calcium entry
CDK	Cyclin dependent kinase
$[Ca^{2+}]_i$	Intracellular Ca^{2+} level
cDNA	complementary acid deoxyribonucleic
CRT	intraluminal calreticulin
DEPC	Diethylpirocarbonate
DHT	Dihydrotestosterone
dNTP	Deoxynucleotide triphosphates
Drg	Differentiation related gene
E_2	17β-estradiol
Ecoli	Escherichia coli
EGF	Epidermal growth factor
EGFR	Epidermal growth factor receptors
ER	Estrogen receptor
FBS	Fetal bovine serum
FGF	Fibroblast growth factor
GZ	Tubuloalveolar glands
HDAC	Histone deacetylase
HGF	Hepatocyte growth factor
HPIN	High-grade prostatic intraepithelial neoplasia
IGF-R	Insulin-like growth factor receptors
HDAC	histone deacetylase
IHC	Imunohistochemistry
ILK	Integrin linked kinase
IL	Interleucine
KGFR	keratinocyte growth factor receptor

M	Month
MAPK	Mitogen-Activated Protein Kinase
MIC	Macrophage inhibitory cytokine
MIF	Macrophage migration inhibitory factor
MMPs	matrix metalloproteinases
mRNA	Messenger ribonucleic acid
MUC	Mucin
nt	Nucleotide
PAP	Acid Phosphatase
PC	Prostate cancer
PCR	Polymerase chain reaction
PI3K	phosphoinositide 3-kinase
PIA	Proliferative inflammatory atrophy
PIN	Prostatic intraepithelial neoplasia
PK	Protein kinase
PSA	Prostate specific antigen
PTEN	Phosphatase and tensin homologue deleted on chromosome 10
PZ	Peripheral zone
qPCR	Quantitative Polymerase chain reaction
RGN	Regucalcin
RNAt	Total RNA
RT	Room temperature
SOCE	Store operated calcium entry
SH	Sullhydryl
SMP-30	Senescence marker protein -30
TNF	Tumor necrosis factor
TSGs	Tumor suppressor genes
TZ	Transitional zone
VEGF	Vascular endothelium growth factor
wt	Wild type
Zn^{2+}	Zinc

List of Figures

List of Tables

Table of Contents

I. Background

1. Anatomy and Pathophysiology of Prostate

1.1. Overview of prostate macro- and micro-anatomy

The prostate is a walnut-sized glandular structure. It is about 4 cm across and 3 cm thick, and lies immediately below the urinary bladder, where it surrounds the initial portion of the urethra (Figure 1).

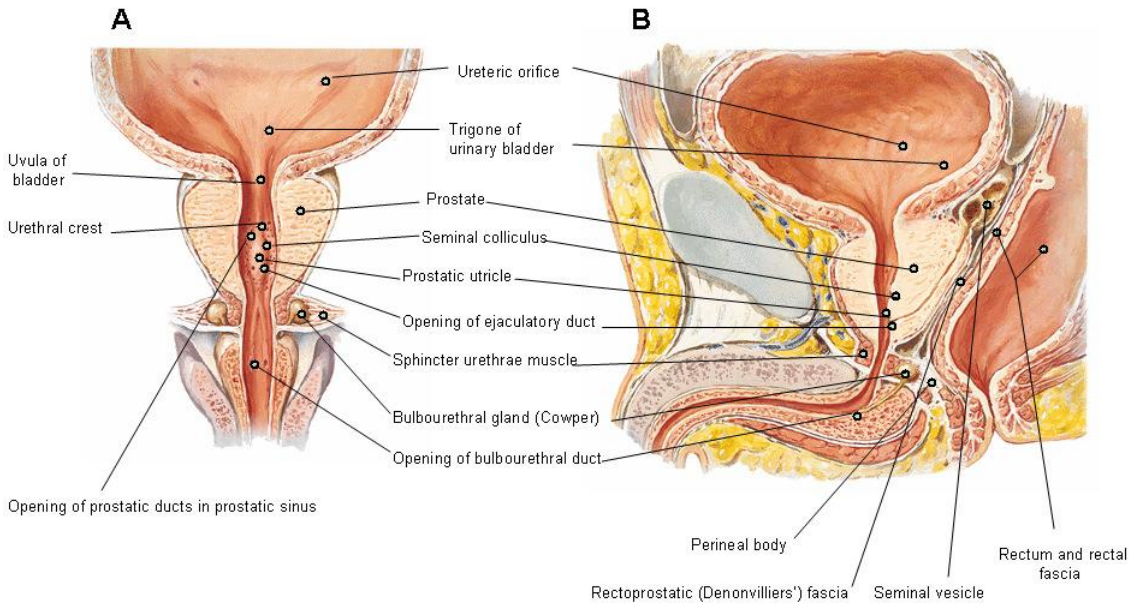

Figure 1: Human prostate anatomy. A- Frontal section with bulbous portion of spongy urethra schematically extended; B- Sagital section (Netter, 1997).

The prostate is enclosed by a fibrous capsule and divided into lobules formed by the urethra and the ejaculatory ducts that extend through the gland. The ducts from the lobules open into the urethra (Graaff, 2002, Joshua et al., 2008). The prostate gland can be divided into five parts: the anterior fibromuscular stroma, a peripheral zone, a central zone, and smaller transition and preprostatic zones (McNeal, 1988, McNeal, 1980, McNeal, 2006) (Figure 2). The peripheral zone (PZ) is the largest region of the prostate, containing approximately 75% of glandular tissue; the central zone (CZ) is the smaller region, comprising approximately 25% of the glandular mass of the prostate and the periurethral area of the gland or the transition zone (TZ) accounts for less than 5% of the prostatic mass (McNeal et al., 1988, Knobil and Neill, 2006). The preprostatic tissue surrounds the urethra and consists of glandular and nonglandular structures,

including a ring of smooth muscle that prevents retrograde ejaculation. The anterior fibromuscular stroma completely covers the surface of the prostate gland and does not contain any ductal structures (Knobil and Neill, 2006).

The glands are irregularly shaped with the epithelium forming folds. Lamellated glycoprotein masses called *corpora amylacea* are a feature of increasing age, becoming progressively calcified to form prostatic concretions (Young, 2002).

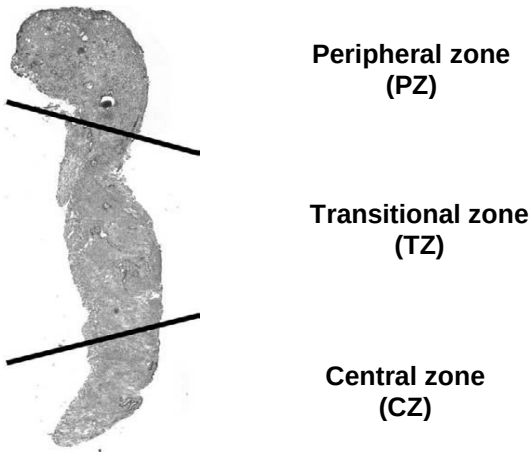

Figure 2: Human prostate needle biopsy specimen showing peripheral zone (PZ), transitional zone (TZ), and central zone (CZ). A variation in ductal and glandular density can be readily observed histologically, although the distinction between the central and peripheral zones can be difficult. The specimen is approximately 6 mm long (Knobil and Neill, 2006).

The prostate gland is composed of two major groups of cells: the epithelial and the stromal cells (Figure 3). Among the epithelial cells there are the secretory cells and basal cells. Neuroendocrine cells, a third type, are present and are believed to be involved in the regulation of prostatic secretory activity and cell growth (Knobil and Neill, 2006).

The secretory cells comprise the exocrine compartment of the prostate epithelium, characterized by columnar luminal cells that produce prostatic secretions, androgen receptor (AR), keratinocyte growth factor receptor (KGFR) and prostate specific antigen (PSA). In the human prostate, basal cells form a continuous layer of cells abutting the basement membrane, and contain insulin-like growth factor receptors (IGF-R), epidermal growth factor receptors (EGFR), and estrogen receptor (ER). The presence of junction-like structures between adjacent basal cells in the human prostate suggests that these cells may form a physical “blood–prostate barrier”, preventing

substances derived from the blood or stroma coming into direct contact with the luminal cells (Knobil and Neill, 2006, Shapiro et al., 2005).

Within the stromal cell population, fibroblastic and smooth muscle cells are thought to produce growth factors that support the development and function of the epithelial cells (Lopez-Otin and Diamandis, 1998).

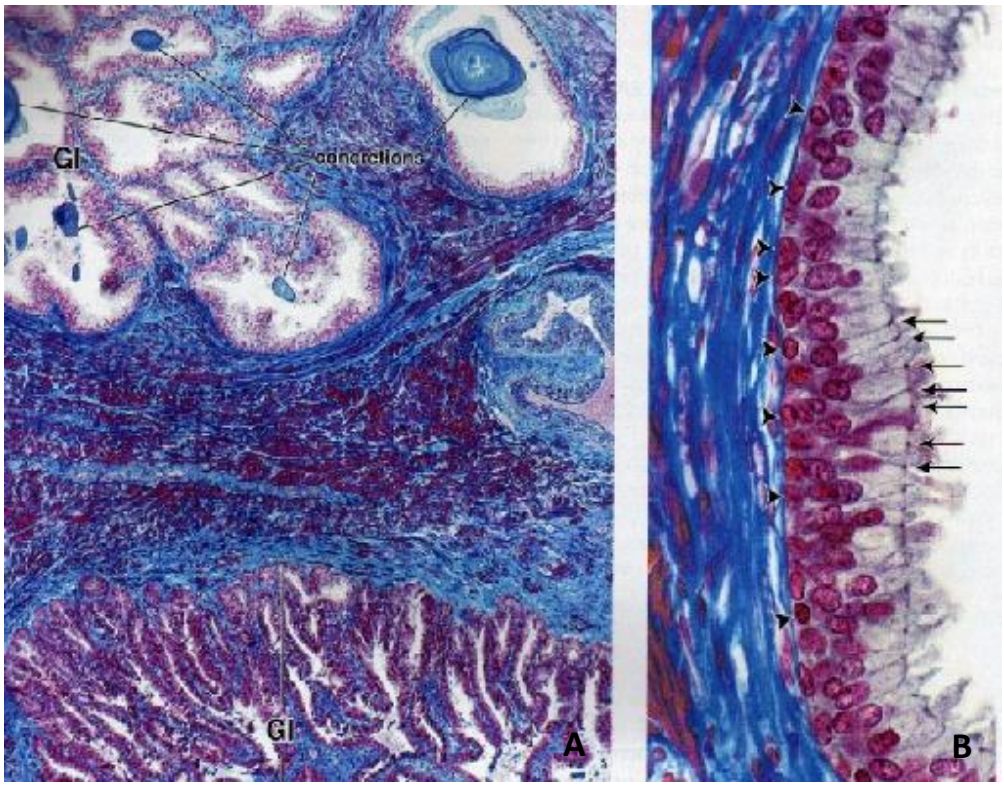

Figure 3: Photomicrograph of human prostate gland. A. This image shows the tubuloalveolar glands (GI) and the fibromuscular tissue that forms the septa between glandular tissue. Within the lumina, various sized prostatic concretions can be seen. The stain utilized for this specimen readily distinguishes the smooth muscle component (stained red) from the dense connective tissue component (stained blue) of the stroma. B. This image shows an area where the glandular epithelium is pseudostratified. The round nuclei adjacent to the connective tissue (arrowheads) belong to the basal cells. Those nuclei that are more elongate and further removed from the base of the epithelium belong to the secretory cells. Note the terminal bars (arrows) that are evident at the apical region of these cells. The red-stained sites within the dense connective tissue represent smooth muscle cells (Ross et al., 2003).

The main function of the prostate gland is to secrete a milky-colored secretion that assists sperm motility as a liquefying agent, and its alkalinity protects the sperm in their passage through the acidic environment of the female vagina. The seminal plasma contains very high concentrations of potassium, zinc (Zn^{2+}), citric acid, fructose, phosphorylcholine, spermine, free amino acids, prostaglandins and enzymes, and

much of this originates from the prostate. The prostate also secretes the enzyme acid phosphatase (PAP), which is often measured to assess prostate function. The prostate discharges make up about 40% of the total volume of the semen (Graaff, 2002).

1.2. Development and hormonal regulation of the prostate gland

Prostate development in the human fetus begins during the 11th to 12th week of gestation as five pairs of epithelial buds emerge from the urethral portion of the urogenital sinus, above and below the entrance of the mesonephric ducts (Figure 4). The five pairs of epithelial buds (anterior, posterior, medial, and two lateral ones) undergo branching to form a lobular arrangement of tubuloalveolar glands surrounded by stroma that encircle the developing urethra and ejaculatory ducts. The top pairs of the buds are composed of epithelia that are believed to be mesodermal in origin and form the TZ of the mature prostate; the lower buds, which form the PZ of the mature prostate, are endodermal in origin (Knobil and Neill, 2006).

The initial outgrowth of the epithelial buds is an androgen-driven process that requires AR expression in the surrounding urogenital mesenchyme to facilitate the reciprocal interactions between the epithelia and mesenchyme. At mid-gestation (~22 weeks of gestational age), the gland consists of small ducts lined by undifferentiated epithelial cells. Increasing levels of maternal estrogen cause squamous metaplasia of the epithelium (i.e., multilayering of the epithelial cells), and at birth the epithelial cells lining the immature glands vary in both the incidence and extent of squamous metaplasia. Upon birth and removal of maternal estrogen, this histological picture is reversed within approximately 4 weeks, and the neonatal gland consists of differentiated pseudostratified epithelia. At puberty, as maturation and growth proceed, the prostate is composed of increasingly complex tubuloalveolar glands arranged in lobules and surrounded by stroma in which fibroblasts, smooth muscle cells, vasculature, nerves, and lymphatics are located. The growth of the pubertal prostate gland is regulated by androgens. The levels of androgens rise during puberty and the prostate gland grows to full size; at maturity androgen levels are maintained, prostate size remains fairly constant, and the organ is considered to be relatively growth quiescent until the fourth decade of life, when growth is reinitiated (Knobil and Neill, 2006).

In the adult, the prostate gland size is maintained through a homeostatic balance between the process of renewal (proliferation) and cell death (apoptosis). This

balance is regulated by hormones secreted by the endocrine system, mainly androgens, of which testosterone is the major circulating form. In humans, the prostatic dihydrotestosterone (DHT) concentration decreases with age, but the concentrations of testosterone and 17β-estradiol (E2) are age-independent (Prins et al., 1996, Shibata et al., 2000). The age-dependent changes in the ratio of serum sex steroid concentration may play a role in benign prostatic hyperplasia (BPH) and prostate cancer (PC) development (Shibata et al., 2000).

The developmental processes between human and rodent are mechanistically similar, the timing is different. Unlike the human prostate, the rodent prostate is rudimentary at birth and branching and differentiation occur postnatally, during the first 15 days of life. During this time, solid prostatic ducts begin to canalize, initially at the urethra, and progressing distally toward the ductal tips. Concurrently, the epithelium undergoes a complex series of changes, including extensive proliferation and segregation and polarization into basal and luminal secretory epithelial cells. Concurrent with epithelial differentiation, the associated mesenchyme differentiates into dense stroma composed of interfascicular fibroblasts and smooth muscle fibers. These processes depend of androgens. Androgenic effects are mediated through ARs located in the stromal and epithelial cells before and during prostatic bud formation. Under the influence of androgens, mesenchymally derived paracrine signals induce epithelial cell differentiation. Estrogens are also present during the developmental period and influence prostatic growth. Although the prostate is highly sensitive to hormones during development, most ductal branching morphogenesis occurs before puberty, when circulating androgen levels are low (Knobil and Neill, 2006).

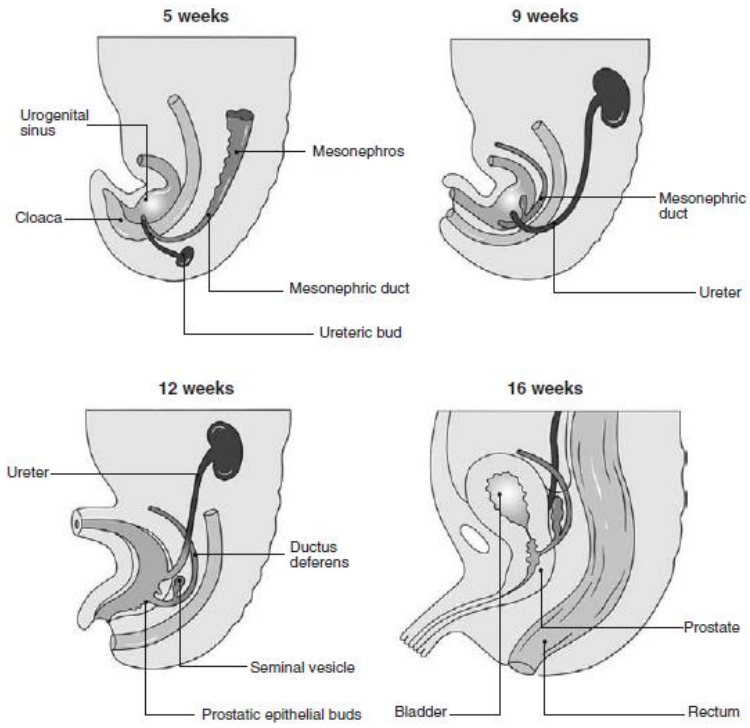

Figure 4: Embryology of the human prostate. The gland develops at the base of the bladder as epithelial buds emerge from the urethral portion of the urogenital sinus, above and below the entrance of the mesonephric ducts (Knobil and Neill, 2006).

1.3. Prostate carcinogenesis

Cancer is a multifactorial disease, which results from the combination of many factors including mutations or polymorphisms of cancer susceptibility genes, environmental agents that influence the acquisition of somatic genetic changes, and several other systemic and local factors including behavior/diet, hormones and growth factors (Ponder, 2001).

PC continues to be a source of considerable morbidity and mortality for men around the world. BPH, a non-malignant overgrowth of the gland, occurs almost exclusively within the TZ of the prostate, and up to 80% of men aged 70–80 years have histological evidence of BPH. Most prostate cancers occur in the PZ, at the dorsal and dorso-lateral side of the prostate; only ≤ 30% of prostate cancers consist of TZ tumors, they have lower biochemical recurrence rates and are less malignant than tumors originating in the PZ (Joshua et al., 2008).

1.3.1. Tumor stages development

PC progresses from precursor lesions, termed prostatic intraepithelial neoplasia (PIN), to overt carcinoma that is confined to the prostate, and finally to metastatic disease, that often results in lethality (Abate-Shen and Shen, 2002) (Figure 5).

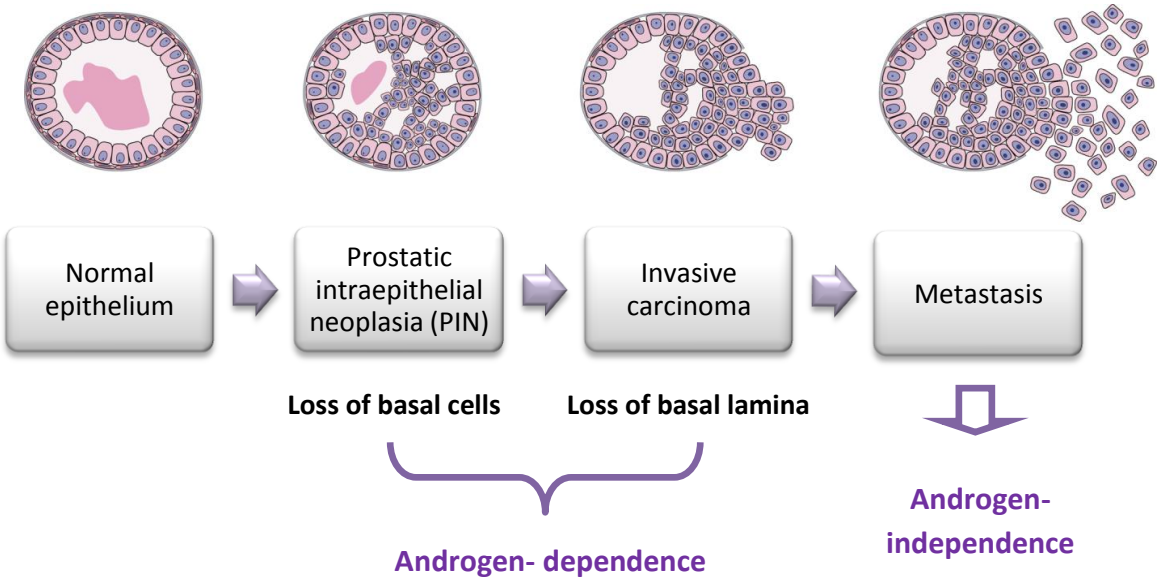

Figure 5: Pathway of human prostate cancer progression (Adapted by Abate-Shen & Shen, 2002).

PC represents a very heterogeneous entity generally composed of a mixture of cells. The presence or absence of AR in cells confers the property of androgen dependency, and androgen-independent cells, respectively. At early stage most of the neoplasic mass is represented by androgen-dependent cells whose proapoptotic potential is regulated by AR. It is well established that this type of cells can be easily induced to undergo apoptotic cell death after androgen ablation. However, associated tumor enrichment with propagating androgen-independent cell population as well as emergence of the new cell phenotypes with enhanced resistance to apoptosis due to genetic transformations will eventually lead to the complete loss of hormone-sensitivity and curability characteristic of advanced stage of cancer (Prevarskaya et al., 2004, Mimeault and Batra, 2006, Schulz and Hoffmann, 2009)

Prostate cancer initiation

Currently, the precursor lesion, high-grade prostatic intraepithelial neoplasia (HPIN) is considered most likely to represent a forerunner to prostate cancer on the basis of pathological, epidemiological and cytogenic evidence (Joshua et al., 2008). An alternative precursor, possibly earlier, is proliferative inflammatory atrophy (PIA). PIA is defined as discrete foci of proliferative glandular epithelium with the morphological appearance of simple atrophy or postatrophic hyperplasia occurring in association with inflammation (Joshua et al., 2008, De Marzo et al., 2007). Prostate dysplastic lesions, in turn, may subsequently give rise to a heterogeneous population of cancer epithelial cells showing aberrant differentiation, unlimited division and a decreased rate of apoptotic cell death (Mimeault and Batra, 2006).

The causes of PC remain poorly understood. Many gene products show deregulated functions. Numerous growth factors and their receptors are also overexpressed during the progression of this hyperproliferative disease. These specific changes of gene expression in epithelial and stromal tumor cells during the different developmental stages of PC notably contribute in enhancing the tumor cell growth, survival, migration and invasiveness. In particular, the activation of multiple developmental signaling cascades including AR, ER, and EGFR, HER's-2, hedgehog and Wnt/b-catenin signaling pathways may confer to them the aggressive phenotypes that are observed in high prostatic PIN grades of malignancy and adenocarcinomas (Figure 6 and 7). More specifically, β-catenin-induced prostate lesions were associated with increasing c-Myc and AR expression levels and an increasing rate of cell proliferation (Mimeault and Batra, 2006).

Moreover, the down-regulation of several apoptotic signaling cascade elements in metastatic PC cells, such as the ceramides and caspases, combined with the enhanced expression of antiapoptotic factors, such as Bcl-2, may also contribute to the survival of tumor epithelial cells (Mimeault and Batra, 2006).

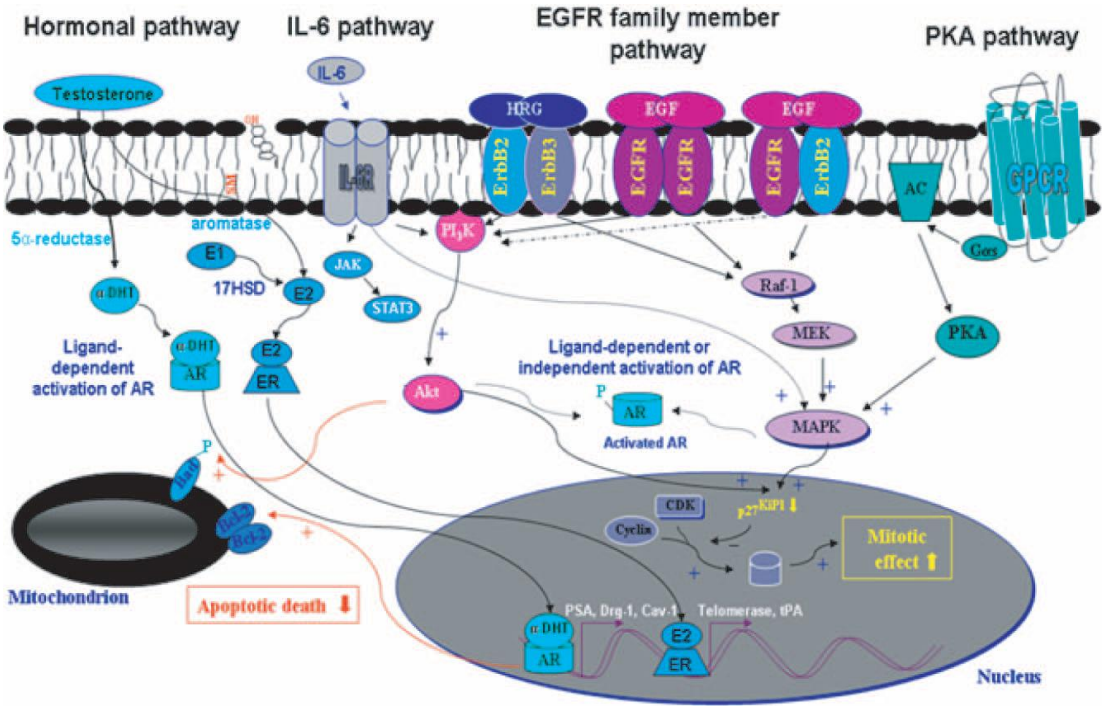

Figure 6: Scheme showing the possible mitogenic and antiapoptotic cascades induced through the androgen receptor (AR), estrogen receptor (ER), epidermal growth factor receptor (EGFR), interleucine-6 (IL-6) and protein kinase A (PKA) signaling pathways. The possible stimulatory effect of growth factor signaling elements on the Mitogen-Activated Protein Kinase (MAPK) and/or phosphoinositide 3-kinase (PI3K) /Akt which may be involved in androgen-dependent and androgen-independent activation of AR in certain PC cells are shown. The enhanced expression levels of AR- and ER-target genes which can contribute to an increase in the tumorigenicity of PC cells are indicated (Mimeault & Batra, 2006).

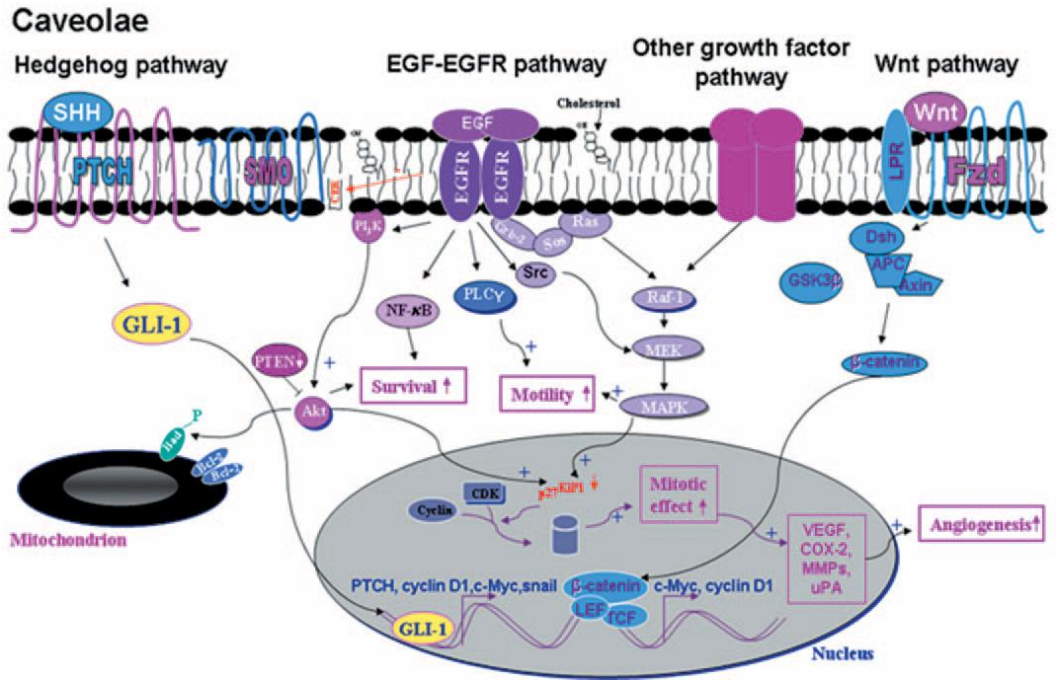

Figure 7: Scheme showing the possible mitogenic and antiapoptotic cascades induced through the epidermal growth factor- epidermal growth factor receptor (EGF–EGFR), hedgehog, Wnt and other growth factor signaling pathway elements co-localized in caveolae. The pathways which are involved in the stimulation of sustained growth, survival and migration of prostatic cancer cells are shown. The enhanced expression levels of numerous tumorigenic genes, including vascular endothelium growth factor (VEGF), interleucine-8 (IL-8), matrix metalloproteinases (MMPs) and uPA, which can contribute to an increase in the angiogenesis, are indicated (Mimeault & Batra, 2006).

Prostate Cancer development and metastasis

Almost all PCs initially develop from secretory epithelial cells of the prostate gland and generally grow slowly within the gland. When the tumor cells penetrate the outside of the prostate gland they may spread to tissues near the prostate, first to the pelvic lymph nodes and eventually to distant lymph nodes, bones and organs such as the brain, liver and lungs. The *in vitro* and *in vivo* characterization of the behavior of numerous human PC cell lines as compared with the normal prostatic epithelial cells, has notably indicated that several oncogenic signaling cascades are involved in regulating the progression from localized and androgen-dependent PC forms into aggressive and androgen independent states (Mimeault and Batra, 2006). Androgen independence is associated with the appearance of new cell phenotypes, characterized by apoptosis inhibition, associated with elevated expression of p53, p21/waf1, BCL-2,

bax and the BCL-2/bax ratio rather than enhanced proliferation (Prevarskaya et al., 2004, Jin-Rong et al., 2004).

The enhanced expression of a variety of growth factors, including EGF, fibroblast growth factor (FGF), hepatocyte growth factor (HGF), nerve growth factor, insulin-like growth factor-1 (IGF-1) and vascular endothelial growth factor (VEGF) appears to assume a critical role in inducing changes in stromal–epithelial cell interactions during PC development (Mimeault and Batra, 2006).

Hence, the oncogenic changes in the tumor stromal– epithelial cells, which may be induced by the activation of distinct growth factor signaling cascades, may confer a more malignant behavior to cancer progenitor cells during the progression from localized PC forms into metastatic states.

1.3.2. Differently-expressed genes

PC cells contain many somatic mutation, gene deletion, gene amplifications and changes in DNA methylation, probably accumulated over a period of several decades (Sciarra et al., 2008).

The progression of epithelial prostate cells from a normal differentiated state, in which proliferation and apoptosis are tightly balanced, to a malignant state involves a combination of events resulting in the activation of oncogenes in addition to the loss of TSGs (tumour-suppressor genes), which critically control aspects of the hallmarks/phenotypes of cancer (Ramsay and Leung, 2009). The enhanced expression of numerous oncogenes and/or a decreased expression of TSGs are induced through the gene amplification and chromosomal deviation or deletion, respectively (Mimeault and Batra, 2006).

TSGs critically regulate the cell cycle, apoptosis, DNA repair, senescence and angiogenesis. TSGs such as p53 and PTEN (phosphatase and tensin homologue deleted on chromosome 10) are important in prostate carcinogenesis (Ramsay and Leung, 2009).

PC cells overexpress several growth factors and their receptors and show enhanced expression and/or activity of a variety of antiapoptotic gene products (Table 1). More specifically, the enhanced expression of cell survival products, such as EGFR (ErbB1), ErbB2 (Her-2/neu), BCL-2, p53, syndecan-1 and clusterin, are among the most frequent genetic alterations observed in metastatic PC (Mimeault and Batra, 2006).

In addition, the up-regulated expression of diverse markers, such as macrophage inhibitory cytokine-1 (MIC-1), Myc, caveolin-1, integrin-linked kinase (ILK), mucin 1 (MUC1), mucin 18 (MUC18) and histone deacetylase 1 (HDAC1), has also been associated with PC progression to more advanced pathological stages (Table 1). On the other hand, inactivating mutations in several TSGs, such as phosphatase PTEN/MMACI and p53, as well as silencing by hypermethylation of distinct invasion suppressor genes, including differentiation related gene-1 (Drg-1), E-cadherin and membrane-anchored serine prostasin, have also been associated with high-grade PINs and a more malignant phenotype of PC cells (Table 1) (Mimeault and Batra, 2006, Meyer et al., 2004). RAS genes activation by point mutations is conspicuously lacking in prostate cancer (Schulz and Hoffmann, 2009).

Similarly, the microarray analyses of differently-expressed genes in early passage androgen-sensitive LnCAP-C33 cells and late passage androgen-independent LNCaP-C81 cells have revealed that several genes, including guanine nucleotide-binding protein Gi, α-1 subunit, cyclin β1, cyclin-dependent kinase-2 (CDK-2), c-myc, c-myc purine-binding transcription factor, macrophage migration inhibitory factor (MIF) and MIC-1, are up-regulated in androgen-independent LnCAP cells (Mimeault and Batra, 2006).

Table 1: Differently-expressed genes in Prostate Cancer (Adapted from Mimeault & Batra, 2006).

Up-regulated genes	**Growth factor receptors**	c-erbB1 (EGFR), c-erbB2 (HER-2/neu), c-erbB3(HER-3), PTCH receptor, IGF-1R, FGFR, VEGFR
	Growth factors	EGF, TGF-α, HB-EGF, amphiregulin, HRG, Wnts, IGF-1, IGF-2, FGFs, HGF, IL-6, VEGF
	Signaling elements	GLI-1, cyclin D1, telomerase, c-myc, caveolin-1, Bcl-2, survivin, clusterin, syndecan-1, NF-kB, ILK, β-catenin, PKC*ε*, HDAC1, COX-2, MMP-2, MUC1, MUC18, S100P, FKBP51, RAS
Down-regulated genes	RB1, p53, PTEN/MMAC, E-catherin, prostasin	

1.3.3. Role of calcium in Prostate cancer

Proliferation and apoptosis are two key processes determining normal tissue homeostasis. Deregulated cell proliferation together with the suppression of apoptosis provides the condition for abnormal tissue growth, which ultimately can turn into uncontrolled expansion and invasion characteristic of cancer. Although in molecular terms proliferation and apoptosis seem to be clearly delineated with the first one relying on cyclin-dependent protein kinases (CDKs), key regulators of the cell division cycle, and the second one on cysteine proteases, the so-called caspases, primary executioners of the programmed cell death. They both involve intense calcium (Ca^{2+}) signaling and Ca^{2+} homeostasis provides critical environment for their unfolding (Prevarskaya et al., 2004).

In general, there are three major Ca^{2+} pools that living cells can utilize for producing various types of cytosolic Ca^{2+} signals: extracellular space, endoplasmatic reticulum, and mitochondria (Abeele et al., 2002). Normal cells maintain a tight regulation over their intracellular Ca^{2+} ($[Ca^{2+}]_i$) activity, with Ca^{2+} entry occurring via one or more pathways including voltage-gated Ca^{2+} channels, receptor-activated channels and non-specific cation channels (Ding et al., 2006).

In PC epithelial cells Ca^{2+} entry from extracellular space is mainly supported by the mechanism called ‘‘capacitative calcium entry’’ (CCE) or ‘‘store-operated calcium entry’’ (SOCE). This mechanism is capable of monitoring the endoplasmatic reticulum Ca^{2+} filling and permits the influx only when endoplasmatic reticulum content essentially decreases. It is mediated via specialized plasma membrane store-operated Ca^{2+}- permeable channels (SOC) (Vanoverberghe et al., 2003).

Progression of PC to the stage of androgen- independence is accompanied by the appearance of new apoptotic-resistance cell phenotypes. One of them is closely associated with overexpression of the common anti-apoptotic oncoprotein, BCL-2 (Prevarskaya et al., 2004, Abeele et al., 2003). BCL2 overexpression in LnCAP prostate cancer epithelial cells results in downregulation of store-operated Ca^{2+} current by decreasing the number of functional channels and inhibiting endoplasmatic reticulum Ca^{2+} uptake (Abeele et al., 2002).

The primary cause of apoptosis induction in response to androgen ablation is sustained elevation of $[Ca^{2+}]_i$ with consequent activation of Ca^{2+}–Mg^{2+}-dependent endonuclease involved in genomic DNA fragmentation (Prevarskaya et al., 2004). Interestingly, androgen ablation not only promotes androgen-dependent PC cell

apoptosis via elevation of cytosolic Ca^{2+}, but increased $[Ca2^{+}]_i$ per se leads to the down-regulation of AR expression (Prevarskaya et al., 2004) (Figure 8).

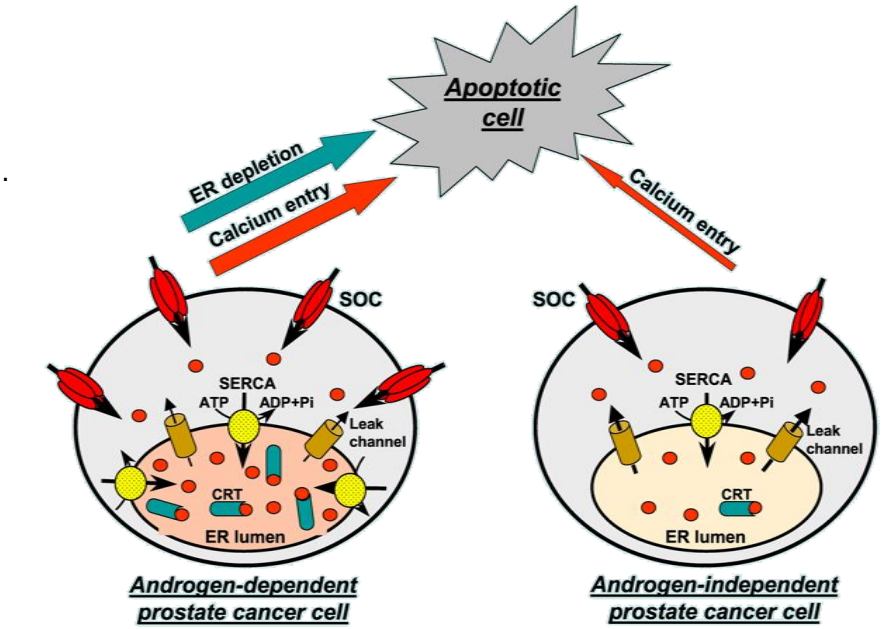

Figure 8: Schematic depiction of the differences in Ca^{2+}-dependent apoptotic pathways in androgen-dependent and androgen-independent prostate cancer (PC) epithelial cells. Left-hand panel presents androgen-dependent PC cell expressing endoplasmic reticulum (ER) leak channels, SERCA pump, intraluminal calreticulin (CRT), and plasma membrane store-operated Ca^{2+} channels (SOCs), whose concert activity provides sufficient ER Ca^{2+} filling and store-operated Ca^{2+} entry to maintain both ER depletion/stress- and Ca^{2+} entry-dependent apoptotic pathways operational. Transition to androgen-independent phenotype (right-hand panel) is associated with significantly lowered ER Ca^{2+} filling due to underexpression of CRT and SERCA pump combined with the enhanced Ca^{2+} leak (shown by thicker arrows via ER leak channels) and decreased store-operated Ca^{2+} entry most probably due to diminished density of SOCs, which eliminates ER depletion/stress-dependent apoptotic pathway and reduces the effectiveness of a Ca^{2+} entry-dependent one (Prevarskaya et al., 2004).

2. Characterization of Regucalcin: molecular biology and physiological roles

Regucalcin (RGN) was discovered in 1978 as a Ca^{2+}-binding protein that does not contain the EF- hand motif of Ca^{2+} binding domain (Yamaguchi and Yamamoto, 1978). Because of its relationship to aging and its molecular mass of 30 kDa, this peptide was also designated senescence marker protein-30 (SMP30) (Fujita et al., 1996a). Kondo et al (2006) found a homology between rat SMP30 and two species of bacterial guconolactonase (GNL: EC 3.1.1.17) derived from *Nostoc punctiforme* and *Zymomonas mobilis*. SMP30 has lactonase activity toward the aldonolactones D- and L-glucono-δ-lactone, D- and L-gulono-γ-lactone, and D- and L-galactono-γ-lactone, with a requirement for Zn^{2+} or Mn^{2+} as a cofactor. The lactonase reaction with L-gulono-γ-lactone is the penultimate step in vitamin C (L-ascorbic acid) biosynthesis (Kondo et al., 2006).

2.1. Gene/mRNA/protein

The rat RGN cDNA , 1,600 bp in length, has an open reading frame of 897 bp, which encodes 299 amino acids with a calculated molecular weight of 35 KDa and an estimated isoelectric point of 5.101 (Fujita et al., 1992). RGN gene has been assigned to the p11.3-q11.2 segment of X chromosome (Fujita et al., 1996a) and it is organized into 7 exons and 6 introns, spanning approximately 17.5 kb (Figure 9). Primer extension analysis revealed two major transcription initiation sites located 101 and 102 bp upstream from the ATG translation initiation codon (Fujita et al., 1996a). The nucleotide (nt) sequence of 5' flanking region showed a TATA-like sequence, a CAAT box, and SP-1 sites at nt -29, -72 and -169 in the promoter region, respectively. In addition to these conventional transcription factor binding sites, were found two clustered Sp1 boxes with AP-2 at nt -2900 and -21376 in the distal promoter region. RGN gene also contains binding sites for two classes of C/EBP transcription factors that are highly expressed in the liver in addition to AP-2, AP-1, GATA-1, and AP-1/GRE (Fujita et al., 1996a).

In terms of RGN mRNA, a wild-type transcript (wt) and two transcript variants (Δ4 and Δ4,5) were identified in human breast and prostate tissue and cells (Figure 10). The Δ4 and Δ4,5 transcripts are likely generated by alternative splicing events and

if translated may encode proteins with 227 and 183 amino acids, respectively (Maia et al., 2009).

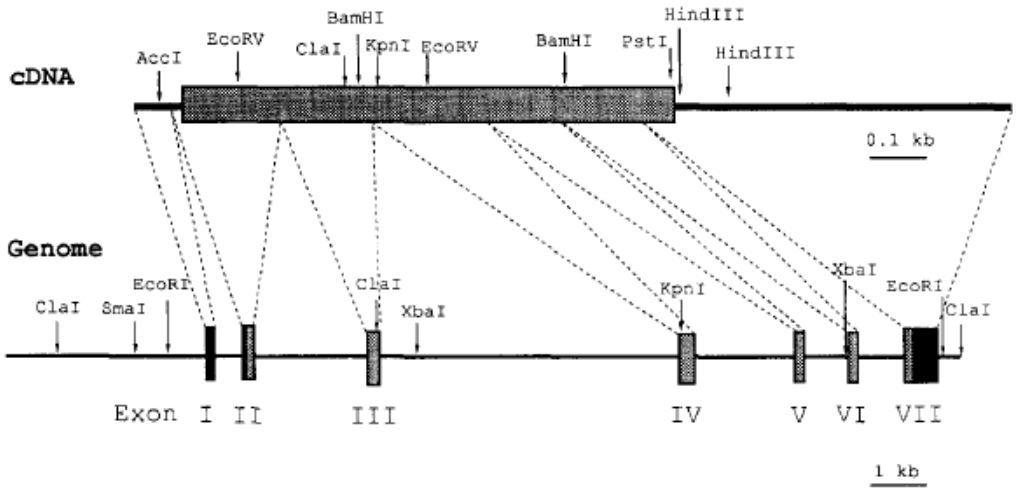

Figure 9: Restriction maps of cDNA and genomic DNA of mouse Regucalcin (RGN), and the genomic organization of mouse RGN. Relevant restriction enzyme sites are indicated in the scheme. Coding and non-coding regions of cDNA are indicated by a gray box and bold solid lines, respectively. Exons are indicated by gray boxes (coding region) and black boxes (non-coding region). Introns are indicated by solid lines. Dashed lines show relationship between the cDNA and the genomic structure of RGN (Fugita et al., 1996).

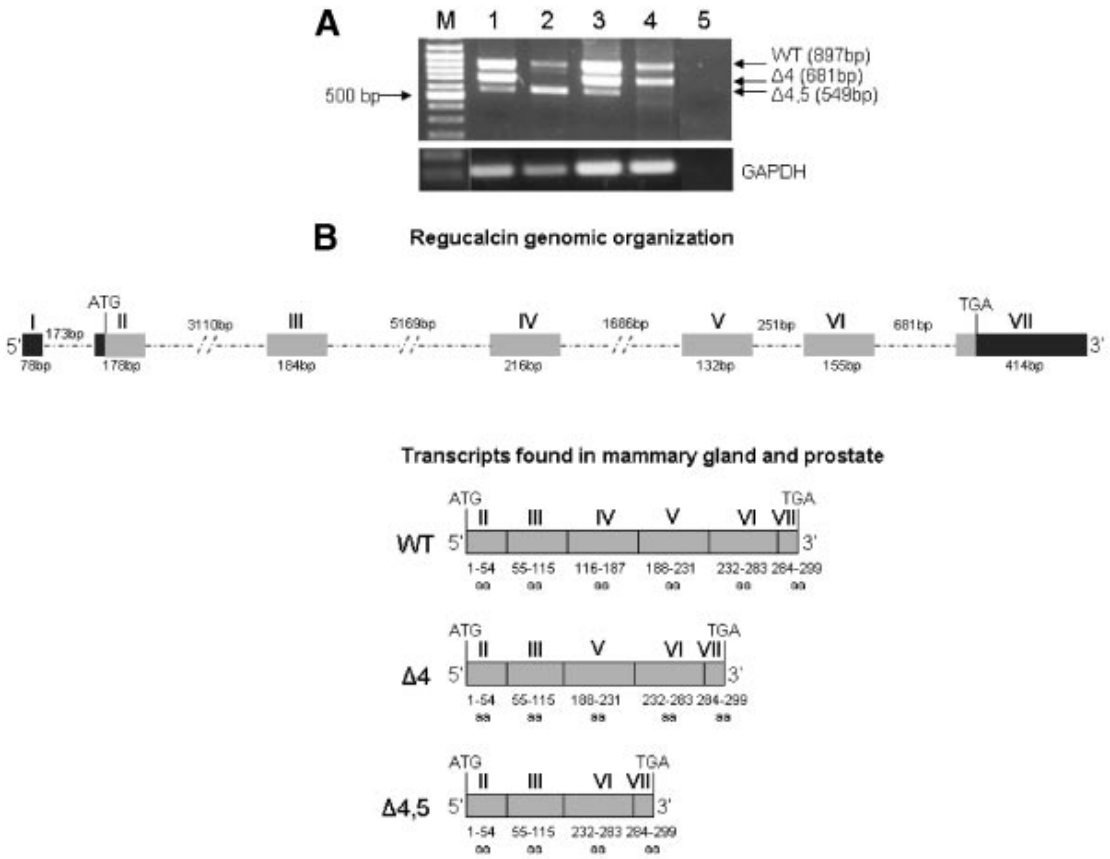

Figure 10: Regucalcin mRNA transcripts in human breast and prostate tissues and cell lines. A: RT-PCR analysis using specific primers spanning the entire coding region of regucalcin. Lane M: DNA Molecular Weight Marker; Lane 1: Non-neoplasic breast tissue; Lane 2: MCF-7 cells; Lane 3: Non-neoplasic prostate tissue; Lane 4: LNCaP cells; Lane 5: Negative control with total RNA not reverse transcribed. B. Diagram of the organization of human regucalcin gene and mRNA variants amplified in RT-PCR reactions. Gray and black boxes indicate coding and noncoding exons, respectively. Dotted lines correspond to introns. Exons are marked with roman numerals. Arabic numerals indicate the number of base pairs per exon or intron, or the number of amino acids (aa) encoded by each exon. WT: wild type regucalcin coding region; Δ4: regucalcin exon 4-deleted variant; Δ4,5; regucalcin exon 4 and exon 5-deleted variant (Adapted from Maia et al, 2009).

RGN is evolutionarily conserved only in higher animals and this gene is not found in yeast (Fujita et al., 1992). The amino acid sequence of mouse RGN showed 94% similarity to rat RGN and 89% to human RGN. In fact, the entire primary structure of RGN is conserved among humans and rodents, suggesting that its complete structure is required for the physiological function of RGN (Fujita et al., 1995, Fujita et al., 1996a)

The primary structure of RGN protein did not show the known Ca^{2+} binding domain, such as an EF-hand motif, and it may represent a calcium binding protein of a novel type.

The Ca^{2+}-binding constant was found to be 4.19 x 10^5 M^{-1} by equilibrium dialysis, and there appears to be six or seven high-affinity binding sites for Ca^{2+} per molecule of protein. The hydropathy profile of RGN showed that there was a hydrophobic sequence in both N-terminal and C-terminal regions of the RGN molecules. However, the protein showed a hydrophilic character as molecule (Shimokawa and Yamaguchi, 1993). RGN molecule contains aspartic acid (24 residues) and glutamic acid (16 residues) which were suggested to be related with Ca^{2+}-binding (Yamaguchi, 2000b).

Very recently, the crystal structure of the human RGN has been determined by X-ray diffraction and the protein has a 6-bladed β-propeller fold, and it contains a single metal ion (Figure 11). Also, both Zn^{2+} and Ca^{2+}-bind to the same metal-binding site in an identical manner. This is interesting, as normally the coordination of Zn^{2+} is quite distinct from that of Ca^{2+} in enzymes. Previous studies, with rat and mouse RGN, have reported that Zn^{2+} is the metal of choice in gluconolactonase activity and Ca^{2+}-in cell regulation and homeostasis (Chakraborti and Bahnson, 2010).

Figure 11: Crystal structure of human Regucalcin (RGN) with calcium (Ca^{2+}) bound. The ribbon structure of RGN displays the six-bladed β-propeller fold with each blade displayed in a rainbow color. The active Ca^{2+} site is shown in the middle of the β-propeller as a purple sphere (Adapted by Chakraborti & Bahnson, 2010).

2.2. Tissue expression and age-specific regulation

In rat tissues, Northern blot and immunohistochemical analyses showed that RGN was specifically expressed in the liver and kidney, where its immunoreactivity was localized in the hepatocytes (in the nuclei and cytoplasm) and the renal tubular epithelia (Fujita, 1999, Fujita et al., 1992). It is expressed in other rat tissues, namely, brain, lung, epidermis, stomach, adrenal gland, ovary, testis, mammary gland and prostate (Fujita et al., 1995, Maia et al., 2008)

In human tissues, RGN was moderately expressed in the pancreas and heart, in addition to the expression in the liver and kidney (Fujita, 1999, Fujita et al., 1992). RT-PCR and immunohistochemical analyses showed that RGN mRNA and protein were expressed in the citosol and nuclei of breast and prostate epithelial cells (Maia et al., 2009).

In livers of rats, RGN decrease androgen-independently with aging. Northern blot analysis showed a marked increase of RGN mRNA in livers of neonatal and young rats. The substantial amounts of protein and transcript were maintained in adults up to 3-6.5 months (M) of age. In the kidney, RGN mRNA and protein started to increase at day 21 and reached near-maximal levels at day 35. The levels of transcript and protein remained high in adults up to 3 M of age. As the aging process progressed to senescent stages, the levels of transcript and protein decreased significantly in the liver and kidney of aged rats. The age-associated decrease of RGN in the liver and kidney may be in a large part controlled at transcriptional levels. The high expression of RGN in the tissue-maturing process and adult suggests that RGN may be required for the maintenance of highly differentiated hepatic and renal functions (Fujita et al., 1996b).

2.3. Regucalcin functions

2.3.1. Intracellular calcium homeostasis

Intracellular Ca^{2+} homeostasis is regulated by plasma membrane (Ca^{2+}-Mg^{2+})-ATPase, microsomal Ca^{2+}-ATPase, mitochondrial Ca^{2+} uptake, and nuclear Ca^{2+} transport in cells (Carafoli, 1987).

RGN is a Ca^{2+}-binding protein involved in the maintenance of $[Ca^{2+}]_i$ homeostasis due to the activation of Ca^{2+} pumping enzymes in the plasma membrane,

endoplasmic reticulum, and mitochondria of many cell types (Takahashi and Yamaguchi, 1999, Yamaguchi, 2000a, Yamaguchi and Daimon, 2005) (Figure 12).

The high-affinity (Ca^{2+}-Mg^{2+})-ATPase is located on the plasma membranes of liver and kidney cells. This enzyme acts as a Ca^{2+} pump to exclude the metal ion from the cytoplasm of the cells. Addition of RGN into the reaction mixture in vitro causes an increase in (Ca^{2+}-Mg^{2+})-ATPase activity in the plasma membranes isolated from rat liver, suggesting a role in the regulation of Ca^{2+} pump activity (Takahasi and Yamaguchi, 1996). Thus, RGN has been shown to bind to liver plasma membrane lipids, and it acts on the sullhydryl (SH) groups which are an active site of (Ca^{2+}-Mg^{2+})-ATPase (Takahashi and Yamaguchi, 1994).

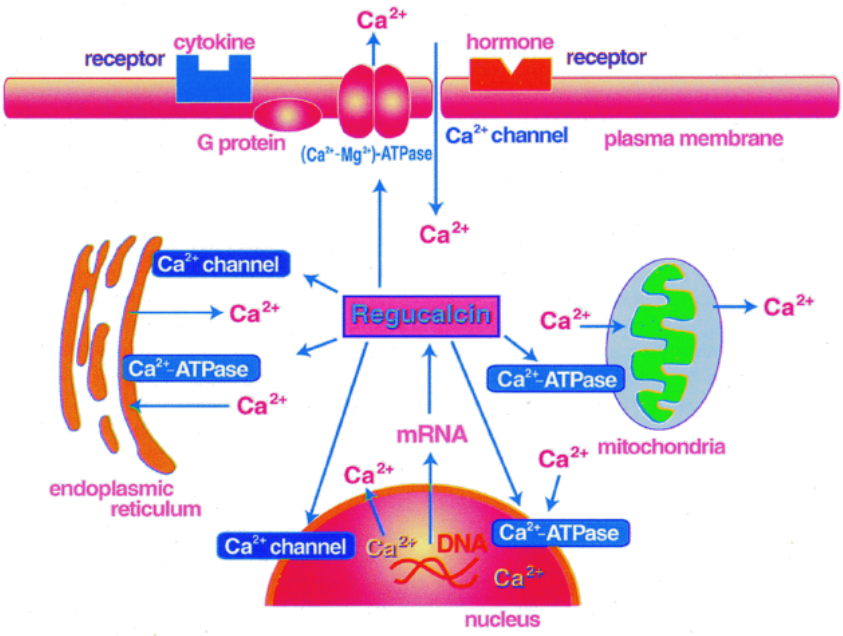

Figure 12: Regulatory role of Regucalcin (RGN) in Ca^{2+} homeostasis of liver cells. RGN increases plasma membrane (Ca^{2+}-Mg^{2+})-ATPase, mitochondrial Ca^{2+}-ATPase and microsomal Ca^{2+}-ATPase activities in rat liver cells. Also, RGN stimulates Ca^{2+} release from the microsomes. RGN has an inhibitory effect on nuclear Ca^{2+}-ATPase and a stimulatory effect on Ca^{2+} release from the nucleus. By this mechanism, RGN may keep the rise of cytosolic Ca^{2+} concentration and nuclear matrix Ca^{2+} levels in the cells that regulate Ca^{2+}- dependent cellular events (Yamaguchi & Daimon, 2005).

Overexpression of RGN causes a remarkable increase in its nuclear localization, and it has suppressive effects on the gene expression of L-type Ca^{2+} channel or calcium polyvalent cation-sensing receptor (CaR) which regulates intracellular Ca^{2+} signaling in the cloned normal rat kidney proximal tubular epithelial NRK52E cells (Nakagawa and Yamaguchi, 2006).

The Ca^{2+} current is one of the most important components in cardiac excitation–contraction coupling. This coupling mechanism is based on the regulation of intracellular Ca^{2+} concentration by Ca^{2+} pump in the sarcoplasmic reticulum of heart muscle. It has been demonstrated that RGN is expressed in rat heart muscle, and that the protein can activate Ca^{2+}-ATPase (Ca^{2+} pump enzyme) in the sarcoplasmic reticulum (Yamaguchi et al., 2002).

RGN mRNA and its protein are expressed in rat brain tissues and brain neuronal cells. The role of RGN in the regulation of Ca^{2+} homeostasis in brain tissues has not been fully clarified, although RGN has been reported to have inhibitory effects on Ca^{2+}-ATPase activity in the microsomes of rat brain tissues. It has been demonstrated that RGN increases Ca^{2+}-ATPase activity in the mitochondria of rat brain tissues, and that the enzyme activity is also elevated in transgenic rats (Yamaguchi et al., 2008).

2.3.2. Calcium-dependent Enzyme Regulation and Intracellular signaling

Protein phosphorylation-dephosphorylation is a universal mechanism by which numerous cellular events are regulated. RGN may play a physiological role in the intracellular control of the hormonal stimulation for phosphorylation and dephosphorylation of many proteins in liver cells (Yamaguchi, 2000a).

RGN has a reversible effect on the activation of various enzymes by Ca^{2+} in liver and kidney cells; it can inhibit the activation of Ca^{2+}/calmodulin-dependent cyclic AMP phosphodiesterase, protein kinase C, and Ca^{2+}/calmodulin-dependent protein kinase (Yamaguchi, 2000a, Tsurusaki and Yamaguchi, 2000).

RGN can inhibit the activation of cyclic AMP phosphodiesterase by Ca^{2+}/calmodulin, responsible for the degradation of the cyclic AMP, and it can inhibit Ca^{2+}/calmodulin dependent protein kinase activity in the cytosol of rat liver and renal cortex cells (Yamaguchi and Tai, 1991, Yamaguchi and Kurota, 1997, Kurota and Yamaguchi, 1997).

Protein kinase C is capable of phosphorylating cytoplasmic proteins. It has been found that RGN inhibits liver cytosolic protein kinase C activity, supporting the view that RGN plays a role in the regulation of Ca^{2+}-dependent cellular functions. Also, RGN has an inhibitory effect on protein kinase C activity in the cytosol of rat kidney cortex (Kurota and Yamaguchi, 1998).

In regenerating rat liver RGN mRNA expression is stimulated through the pathway of signaling mechanism concerning CaM kinase, protein kinase C, and

thyrosine kinase increased by partial hepatectomy. RGN inhibits the activities of various nuclear protein kinases and phosphatases, and it inhibits nuclear DNA and RNA synthesis in proliferative liver cells. This protein may have an important role in the regulation of nuclear function in proliferative liver cells (Yamaguchi and Kanayama, 1995) (Figure 13).

RGN plays an inhibitory role in the signaling pathway which is mediated through Ca^{2+}-dependent protein kinases in liver and kidney cells.

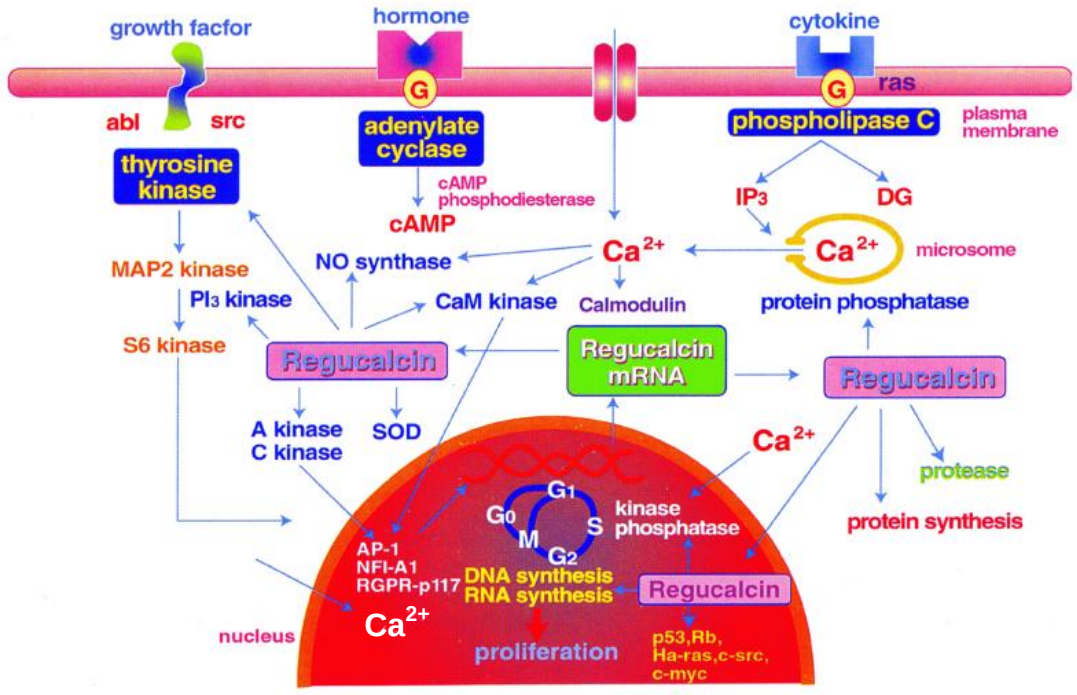

Figure 13: Role of Regucalcin (RGN) in the regulation of nuclear functions in regenerating rat liver. RGN mRNA expression in liver cells is stimulated through the pathway of signaling mechanism concerning protein kinases increased by partial hepatectomy, and RGN reveals an inhibitory effect on nuclear DNA and RNA synthesis in the proliferative cells of regenerating liver. RGN may suppress the proliferation of liver cells (Yamaguchi and Daimon, 2005).

2.3.3. Protease regulation

RGN has been shown to activate neutral cysteinyl-protease including calpain in the cytosol of rat liver and kidney cortex cells, in a mechanism independent of Ca^{2+} (Yamaguchi and Nishina, 1995) .The ability of calpain to alter the limited proteolysis, the activity or function of numerous cytoskeletal proteins, protein kinases, receptors, and transcription factors suggests an involvement of the protease in various Ca^{2+}-regulated cellular functions. If RGN activates cysteinyl proteases including calpain, it may be implicated in many cellular functions which are regulated by cyteinyl proteases in liver cells (Yamaguchi, 2000a).

2.3.4. Apoptosis and cellular proliferation

RGN has been shown to have a suppressive effect on cell proliferation. The expression of RGN mRNA is enhanced in the proliferative cells after partial hepatectomy in rats (Yamaguchi and Kanayama, 1995) and the translocation of RGN into the nucleus is increased in regenerating rat liver. Endogenous RGN has been shown to prevent the enhancement of nuclear DNA and RNA synthesis in regenerating rat liver, suggesting that the protein regulates proliferation of liver cells (Tsurusaki et al., 2000, Tsurusaki and Yamaguchi, 2002, Tsurusaki and Yamaguchi, 2003b). Endogenous RGN has been shown to have a suppressive effect on cell proliferation and DNA synthesis in the cloned rat hepatoma H4-II-E cells overexpressing RGN (Misawa et al., 2002). RGN is found to bind nuclear proteins or DNA in vitro, and their overexpression suppresses the expression of oncogenes c-myc, Ha-ras, or c-src and enhances the expression of TSGs p53 and Rb in the cloned hepatoma cells (Tsurusaki and Yamaguchi, 2003a). Cell proliferation is suppressed in NRK52E cells overexpressing RGN *in vitro* (Nakagawa and Yamaguchi, 2005).

The suppressive effect of RGN on cell proliferation is partly mediated through the regulation of intracellular signaling-related factors. RGN enhances p21 mRNA expression, which participates in cell cycle arrest and suppresses IGF-I mRNA expression, a growth factor in cell proliferation, in the hepatoma cells. It suppresses the expression of p53 mRNA in the cloned rat hepatoma H4-II-E cells. p53 is known to stimulate p21 mRNA expression to induce cell-cycle arrest (Yamaguchi and Daimon, 2005). RGN downregulates several proteins involved in cell proliferation such as Ca^{2+}-dependent protein kinases, tyrosine kinases, protein phosphatases and NO synthase (Yamaguchi, 2000a, Yamaguchi, 2005).

Contrastingly, there are also reports describing RGN roles suppressing cell death and apoptosis.

RGN promotes Akt activation in HepG2/RGN cells, which has an anti-apoptotic effect in many different types of cells, in the presence or absence of Tumor necrosis factor -α (TNF-α) plus actinomycin (ActD). This effect was dependent on CaM (Matsuyama et al., 2004). In addition, SMP30-KO mice hepatocytes were more susceptible to apoptosis induced by TNF-α plus ActD than hepatocytes from wt mice (Ishigami et al., 2002, Maruyama et al., 2010).

RGN regulates Ca^{2+} kinetics involved in the plasma membrane Ca^{2+}-pumping activity of HepG2 and LLC-PK1 cells showing that RGN could rescue cells from an apoptotic death induced by a high intracellular Ca^{2+} level ($[Ca^{2+}]_i$) (Kondo et al., 2004).

It has been demonstrated that RGN overexpression has a preventive effect on cell death and apoptosis induced by LPS or other intracellular signaling-related factors in the cloned rat hepatoma H4-II-E cells (Izumi and Yamaguchi, 2004).

In NRK52E cells RGN overexpression has a suppressive effect on cell death and apoptosis induced by various apoptotic factors. Bcl-2 is a suppressor in apoptotic cell death. Overexpression of RGN caused a remarkable elevation of Bcl-2 mRNA expression in NRK52E cells, and it slightly stimulated Akt-1 mRNA expression in the cells (Nakagawa and Yamaguchi, 2005).

It also plays a profound role in rescuing cells from cellular injuries such as apoptosis and hypoxia (Ishigami et al., 2002).

2.4. Regucalcin expression in prostate pathophysiological state.

Very recently, Maia et al (2008) demonstrated for the first time that RGN mRNA and protein are expressed in the citosol and nuclei of rat and human prostate epithelial cells (Maia et al., 2008). Moreover, it was described a diminished expression of RGN protein in human prostate cancer cases, which was correlated with tumor differentiation (Maia et al., 2009).

Primary prostate cancers are dependent of androgenic stimulation and a reduction of RGN mRNA expression was observed in LnCAP cells in response to DHT stimulation (Maia 2009).

II. Objectives

The present project aims to determine the role of RGN on the expression of oncogenes and TSGs in prostate cell lines. To achieve this goal, the following specific objectives were delineated:

1. Characterize RGN expression in prostate tissues and cell-lines: different post-natal ages; cell-lines and immunolocalization in tissue sections;

2. Construction of expression vectors for wt RGN and, Δ4 and Δ4,5 variants;

3. Culture and transfection of non-neoplasic and neoplasic prostate cell lines;

4. Confirmation of RGN-overexpression in non-neoplasic and neoplasic prostate cell lines;

5. Determine the effect of RGN on the expression of oncogenes and TSGs in non-neoplasic and neoplasic prostate cell lines.

III. Material and Methods

1. Reverse Transcriptase –Polymerase Chain Reaction- RT-PCR

RT-PCR consists in three procedures: RNA extraction, cDNA synthesis and polymerase chain reaction (PCR) which permits the analysis of patterns of gene expression.

1.1. Total RNA extraction

Total RNA (RNAt) was extracted using TRI reagent (Sigma) according to the manufacturer's instructions. TRI is a mixture of guanidine isothiocyanate and phenol which dissolves DNA, RNA and proteins.

An appropriate volume of TRI-Reagent was added to cells or tissues, which were homogenized using an Ultra turax T25 basic (IKA ® WERKE) and incubated for 5 minutes (min) at room temperature to dissociate nucleoprotein complexes. 200 µl of chloroform (Sigma) per ml of TRI reagent was added, and the sample was vortexed vigorously for 15 seconds and incubated for 2-10min at room temperature (RT). After that incubation period, samples were centrifuged (12.000g for 15min at 4ºC) and the mixture was separated into three distinct phases. The upper, aqueous phase, which contains RNA, was transferred to a fresh tube and 500 µl of isopropanol per ml of TRI reagent used was added. Samples were incubated for 5-10min at RT and centrifuged at 12.000g for 10min at 4ºC. The supernatant was removed and the RNA pellet washed with 1ml of 75% DEPC-Ethanol (at -20ºC) per ml of TRI reagent used. After centrifugation at 7.500g for 5min at 4ºC, the supernatant was removed and the wash step was repeated. Finally, the resultant RNA pellet was dried at 55-60ºC and ressupended in an appropriate volume of DEPC-treated water (Sigma).

In order to assess the quantity and integrity of total RNA, its optical density was determined by measuring absorbance at 260 and 280 nm and the corresponding ratio was calculated (Pharmacia Biotech, Ultrospec 3000). RNA extracts were also inspected by agarose gel electrophoresis with ethidium bromide using an appropriate photography and image acquisition equipment (Vilber Lourmat).

1.2. cDNA synthesis

cDNA synthesis is the enzymatic conversion of RNA to a single-stranded cDNA template. 1 µg of RNAts were reverse transcribed into cDNA. Firstly, RNAt was incubated at 65ºC for 5min with dNTP mix, random hexamer primers (Table 2), and DEPC water to a final volume of 12 µl.

After a brief centrifugation, mixtures were incubated for 2min at 37ºC with 5x First-Strand Buffer, RNase OUT and DTT (Table 2). 200U of M-MLV RT (Invitrogen) was added, mixed by pipetting and incubations proceeded during 10min at 25ºC, and 50min at 37ºC. The reaction was stopped by heating at 70°C for 15min, and stored at -20ºC. All incubation steps were performed in a thermal cycler (Px2 Thermo Hybaid).

Table 2: Reagents and volumes used in each cDNA synthesis reaction.

Reagent	Volume (µl)
Random Hexamer Primers (Invitrogen)	2
dNTP Mix (10 nM; Amersham, GE Healthcare)	1
5x First-Strand Buffer (Invitrogen)	4
DTT (0,1 M; Invitrogen)	2
RNaseOUT-Recombinant Ribonuclease Inhibitor (40 U/µL; Invitrogen)	1

1.3. PCR

PCR permits DNA amplification. Components of a standard PCR reaction are: termostable DNA polymerase, DNA template, primers, deoxynucleotide triphosphates (dNTPs), Buffer and $MgCl_2$, and consists in three steps: denaturation, annealing and extension.

PCR reactions were carried out using 1µg of synthesized cDNA in a 50µl reaction containing: 5µl of Buffer, 10mM dNTPs (Amersham), 50mM of each primer pair specific to different cDNA, Taq DNA polymerase and sterile water. All PCR reactions were carried out in a thermal cycler (Px2 Thermo Hybaid).

To amplify oncogenes and TSGs cDNAs, was used 0,125U DreamTaq™ Polymerase (Fermentas) and DreamTaq Buffer (KCl, $(NH_4)_2SO4$ and $MgCl_2$ 20 mM).

The housekeeping gene 18S was amplified as an internal control. Details of primers sequences and amplification cycles for the studied genes are listed in table 3.

For the amplification of wt, Δ4 and Δ4,5 RGN was used an enzyme with proofreading activity, Extensor (ABgene) 2,5U and 10 x Extensor Buffer 1 (22.5mM $MgCl_2$). To amplify cDNA sequences allowing subcloning in expression vectors, RGN specific PCR primers were modified to contain NheI and XhoI recognition sites, respectively in 5' and 3' prime-ends. Details of primers sequences and amplification cycle are indicated in Table 4.

The amplified PCR fragments were separated by agarose gel (1%) electrophoresis with ethidium bromide and visualized using an appropriate photography and image acquisition equipment (Vilber Lourmat).

Table 3: Primers sequences, amplicon size and cycling conditions for amplification of oncongenes (BCL2, Ha-ras and c-myc), tumor suppressor genes (p53 and RB1) and 18S cDNAs.

Primers	Sequence	Amplicon size (bp)	PCR Cycle
hHaRASfw748 **hHaRASrv947**	5´TGCTCTCCTGACGCAGCACAA3´ 5´GCTGGGGTTCCGGTGGCATT3´	219	94ºC-3min 94ºC-30s 50ºC-30s 72ºC-30s } 40x 72ºC-5min
hBCL-2fw1069 **hBCL-2rv1529**	5´CGGAGGCTGGGATGCCTTTGT3´ 5´GAGCCACACGAAGCGGTGCT3´	480	94ºC-3min 94ºC-30s 55ºC-30s 72ºC-45s } 40x 72ºC-5min
hMycfw334 **hMycrv548**	5´TCCGCAACCCTTGCCGCATC3´ 5´CGCGGGAGGCTGCTGGTTTT3´	234	94ºC-3min 94ºC-30s 56ºC-30s 72ºC-30s } 40x 72ºC-5min
hRB1fw1626 **hRB1rv2479**	5´TGGCGTGCGCTCTTGAGGTT3´ 5´TAGGGGGCCTGGTGGAAGCA3´	873	94ºC-3min 94ºC-30s 55ºC-30s 72ºC-30s } 40x 72ºC-5min
hP53fw191 **hP53rv750**	5´CACTGCCATGGAGGAGCCGC3´ 5´GGAGGGGCCAGACCATCGCT3´	579	94ºC-3min 94ºC-30s 55ºC-30s 72ºC-60s } 40x 72ºC-5min
18sfw **18srv**	5'AAGACGAACCAGAGCGAAAG3' 5´GGCGGGTCATGGGAATAA3´	152	94ºC-2 min 94ºC- 30 s 56ºC- 30 s 72ºC- 30 s } 25x 72ºC- 5 min

Table 4: Primers sequences, amplicon size and cycling conditions for amplification of wt, Δ4 and Δ4,5 RGN cDNAs.

Primers	Sequence	Amplicon size (bp)	PCR Cycle
hRGNfwNhe1 **hRGNrevXho1**	5'TGAGCTAGCCTGCGACCATGTCTTCCATTA3´ 5´CCTGCTCGAGTCCCGCATAGGAGTAGGGAC3´	WT-897 Δ4-681 Δ4,5-549	94ºC-5min 94ºC-30s 60ºC-30s 68ºC-60s 68ºC-5min 40x

2. Cloning of RT-PCR DNA fragments

Cloning involves construction of hybrid DNA molecules that are able to self-replicate in a host cell. In this procedure, the plasmid and the DNA fragment are engineered to be linear molecules with termini compatible to be joined by ligation.

The PCR products obtained from liver cDNA amplification were cloned in pGEM-T easy vector (Promega) and sequenced to confirm the identity of the amplicons.

2.1. PCR products purification

The cDNAs encoding human wt, Δ4 and Δ4,5 RGN were purified from agarose gel bands using the Nuleospin extract II, PCR clean-up/ Gel extraction kit (MACHEREY-NAGEL) according to the manufacturer's instructions.

After running the agarose gel, the gel band was excised from the gel and weighted. For each 100 mg of gel, 200 µl of Binding buffer NT was added. After incubation of the mixture at 50ºC to dissolve the gel, the column was placed into the collecting tube; the sample was loaded with 600 µl of wash buffer NT3 and centrifuged for 1min at 11.000g. The flow was discarded and the column was placed back into collecting tube. The centrifugation was repeated for 2min to completely dry membrane. Finally, the column was placed into a clean tube, 20-25 µl of elution buffer NE was added and the sample was incubated at room temperature for 1min. The DNA was collected by centrifugation for 1min at 11.000g and stored at 4ºC. The purification efficiency was confirmed by electrophoresis on a 1% agarose gel.

2.2. Ligation of inserts into pGEM®-T Easy Vector

DNA fragments were ligated to pGEM-T Easy Vector by adding: 0.5 µl of pGEM®-T Easy Vector, 2.5 µl of 2x Buffer, 1.5 µl of purified DNA, 0.1-1U of T4 DNA ligase (Promega) and sterile water to a final volume of 10 µl. The reactions were incubated at 4ºC and ligation performed overnight.

2.3. Transformation of competent bacteria XL1B

1 µl of the ligation reaction was added to 100 µl of competent *Escherichia coli (E.coli)*, strain XL1B and incubated on ice for 35-40min. The next step was to perform a heat shock by incubating for 2min at 42ºC. The bacterial cells were immediately plated in agar (USB) plates with IPTG (0.5mM), X-Gal (80 µg/ml) and Ampicilin (100 µg/ml), in sterile conditions. The plates were incubated at 37ºC overnight.

2.4. Culture of bacteria in liquid medium

White colonies were picked and placed in 15 ml culture tubes containing approximately 4ml of LB Broth medium supplemented with amplicilin (100 µg/ml), in sterile conditions. Cultures were incubated overnight at 37ºC in an orbital shaking incubator (200 rpm; ARABAL Agitorb 200E).

2.5. Purification of DNA plasmid

To purify plasmid DNA the kit Wizard® Plus Minipreps DNA Purification System (Promega) was used, according to the manufacturer's instructions.

The bacterial cells from overnight cultures were harvested by centrifugation at 10.000g for 5min. 250 µl of Cell Resuspension Solution was added. After vortex, 250 µl of Cell Lyses solution was added, mixed by inversion and incubated until suspension clears. 10 µl of Alkaline protease solution was added, mixed and incubated for no longer than 5min. 350 µl of Neutralization solution was added and mixed. After centrifugation of 14.000g for 10min, lysate was transferred to spin column. Another centrifugation was done at 4.000g for 1min. Column Wash Solution was added in two steps, first 750 µl and centrifugation at 14.000g for 1min and finally was added 250 µl with centrifugation at 14.000g during 2min. The column was transferred into a fresh

tube, and was added 100 µl of Nuclease- free water. The purified DNA was collected by centrifugation at 14.000g for 1min, and stored at -20ºC.

2.6. Digestion of plasmid DNA

To confirm the insertion of wt, Δ4 and Δ4,5 RGN cDNAs in the pGEM-T Easy Vector, plasmids were digested with Eco RI (Takara), which allows fragments release. The digestion reaction contained: 2.5 µl of purified plasmid DNA, 1 µl of 10x Buffer, 7,5 U of Eco RI and sterile water to a final volume of 10 µl. After incubation at 37ºC for 1h30min, digestion products were separated by electrophoresis on a 1% agarose gel with ethidium bromide.

2.7. DNA Sequencing

The identity and orientation of fragments was confirmed by Sanger sequencing Method performed at STABVIDA custom services (Oeiras, Portugal) (Atachment).

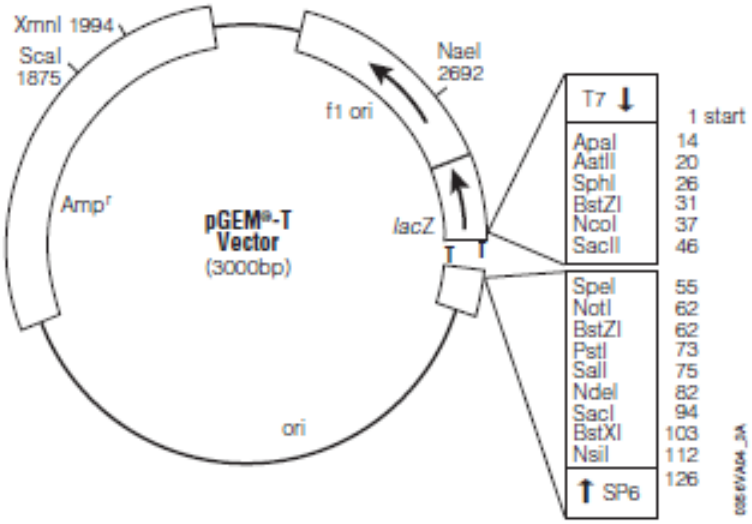

Figure 14: pGEM®-T Easy vector Map (Adapted from Promega, pGEMR-T and pGEMR-T Easy Vector Systems Manual- TM042).

3. Sub-cloning procedure

pIRES2-AcGFP1 (Figure 15) is a bicistronic vector designed for the simultaneous expression of a novel green fluorescent protein (AcGFP1) and a protein of interest from the same transcript in transfected mammalian cells (Clontech).

The cDNAs encoding human wt Δ4 and Δ4,5 RGN, were isolated from pGEM-T easy vector by double-digestion with NheI and XhoI (Takara) and cloned into the pIRES2-AcGFP1 expression vector digested with the same restriction enzymes. Digestions were performed using 1 µl of each restriction enzyme, 5 µl of Buffer M, 30 µl of pGEM-T with RGN fragments or 3 µl pIRES-AcGFP1 vector and sterile water to a final volume of 50 µl. Reactions were incubated at 37ºC for 1h30min and the enzyme inactivated at 60ºC, 15min.

After digestion, both reactions were run in an agarose gel, the fragments of interest (pIRES linearized and RGN fragments) were cut from the gel and purified with kit NucleoSpin Extract II, as described above.

Ligation of RGN cDNAs in pIRES-AcGFP1 was carried out using 1 µl of linearized and purified pIRES-AcGFP1 vector, 3 µl of RGN purified fragment, 1 µl 10x buffer, 0.1-1 U T4 DNA Ligase and sterile water in a 10µl reaction. After overnight incubation at 4ºC, 1µl of ligation products were used to transform *E.coli* XL1B competent cells. The following procedures till plasmid purification were the same as described in 3.3, 3.4 and 3.5, except that in this case was used culture media supplemented with kanamycin (50 µg/ml).

The resultant recombinant plasmids designated as pIRES-AcGFP1/RGNwt, pIRES-AcGFP1/RGNΔ4 and pIRES-AcGFP1/RGNΔ4,5, were double-digested with XhoI and NheI to confirm the presence of the insert in the expression vector and separated by electrophoresis on a 0.8% agarose gel with ethidium bromide.

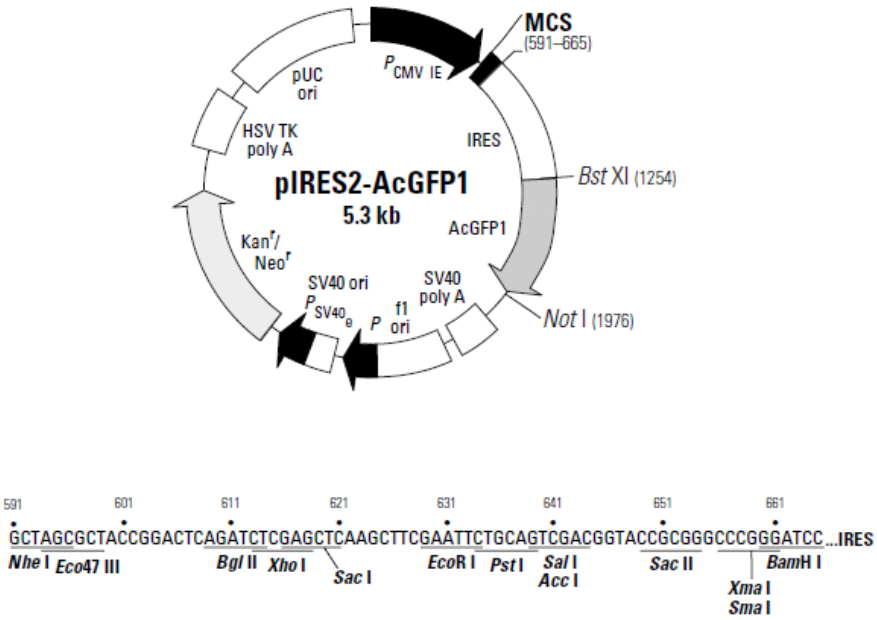

Figure 15: pIRES2-AcGFP1 vector Map and Multiple cloning site (MSC) (Adapted from Clontech, pIRES2-AcGFP1 vector protocol- Cat. No. 631601).

4. Protein Extraction

Total protein from tissues or cells was extracted using RIPA Buffer, which contains RIPA (150 mM NaCl; 1% Nonidet-P40 substitute; 0,5% Na-deoxycholate; 0,1% SDS; 50 nM Tris ; 1mM EDTA), 1% Protease inhibitor cocktail and 10% PMSF.

An appropriate volume of RIPA Buffer was added to cells and the mixture was incubated during 20min in ice and centrifuged (12000 rpm for 20min at 4ºC). The supernatant was removed to new tubes and stored at -80ºC. Total Protein was quantified using the Bradford Method (Bradford, 1976).

5. Western Blot Analysis

Total proteins extracts were resolved by SDS-PAGE (Table 5) and electrotransferred to a PVDF membrane (Amersham), previously activated in methanol, water and electrotransferation Solution (10mM CAPS in 10% methanol, pH=11), at 750mA and 4ºC for 30min. Membranes were blocked in Tris-buffered saline with Tween 20 (TBS-T, Applichem, Darmstadt, Germany) containing 5% milk (Regilait, France) for 1h. The membrane was then incubated overnight at 4ºC with a mouse

monoclonal primary antibody anti-rat RGN (Abcam, ab81721, 1:200). After washing in TBS-T, the membrane was incubated for 1h with goat polyclonal antibody against mouse IgG (Abcam, ab7069, 1:12000). At the end, the membrane was again washed in TBS-T, air dried, and incubated with ECF substrate (Amersham) for 3min and visualized on the Molecular Imager FX Pro plus MultiImager (Biorad, Hercules, USA).

Table 5: Resolving and stacking gel composition used in SDS-PAGE.

Resolving gel	Stacking gel
4,15 mL acrilamide (40%)	1,75 mL acrilamide (40%)
4,15 mL Tris-HCl 1.875M pH 8.8	1,25 mL Tris-HCl 1.25M pH 6.8
1,8 ml Water	6,9 ml Water
0,1 ml SDS 10%	1 ml SDS 10%
125µL PSA	250 µL PSA
7,5 µL TEMED	7,5 µL TEMED

6. Immunohistochemistry

Immunohistochemistry (IHC) is used in protein analysis in tissue and is based on the ability of antibodies to bind a tissue antigen. RGN was detected by IHC in formalin-fixed, paraffin-embedded human prostate sections. These sections were deparaffinized with xylene during 5min and rehydrated using graded ethanol series, absolute, 95% and 80% ethanol. Slides were gently rinsed in running tap water for 30 seconds, and placed 20min in a heated citrate-bath. Slides were washed in water for 5min. Sections were incubated with 0.3% hydrogen peroxide for 20min to inactivate the endogenous peroxidase. Slides were rinsed with Phosphatase Buffered saline serum (PBS, 0,01 M, pH=7,4) with Tween 20 (Amresco, USA), washed in a PBS bath for 5min and incubated with 0,01 % Digitonin for 5min to permeabilize. The wash step with PBS was repeated. Non-specific protein binding was eliminated by incubation with PBA and 0,3 M glycine for 30min at RT. Sections were then washed with PBS and incubated overnight at 4ºC with a mouse monoclonal primary antibody anti-human Regucalcin (Abcam, ab81721) diluted 1:50 in PBS containing 1% BSA. After primary antibody incubation slides were washed with PBS for 5min, and incubated for 1h with biotinylated goat anti-mouse IgG (Abcam, ab7069, 1:400). Sections were washed in

PBS for 5 min at RT, incubated with a Rabbit ExtrAvidin Peroxidase reagent (Sigma) for 30 min, and then washed in PBS for 5min. The color development was carried out using 0.05% 3,3- diaminobenzidine hydrochloride (DAB, Sigma) and 0.0006% hydrogen peroxide in TBS. Sections were counterstained in Mayer's hematoxylin for about 10 seconds. Slides were rinsed under running tap water. Sections were dehydrated, cleared, and mounted with Entellan® neu mounting media (Merck, Germany). For negative control, sections were incubated in PBS containing 1% BSA omitting the primary antibody. Images of the slides were observed in a microscopy (Primo Star- Zeiss) and captured with a camera (PomerShot A640- Canon).

7. Cell culture

The human prostate cancer cell lines PC3, LnCAP and the immortalized normal prostate epithelial cell lines PNT1A and PNT2 were cultured in RPMI 1640 (Invitrogen), in an incubator at 37ºC equilibrated with 5% CO_2. All cultures were supplemented with 10% FBS (Biochrom, Berlin, Germany) and 1% penicillin/streptomycin (Invitrogen).

8. Transient transfection assay

For transient transfection PC3, LnCAP, PNT1A and PNT2 cells growth in a 24 well plate in a lamella to approximately 40% confluence. pIRES-AcGFP1/ RGNwt, pIRES- AcGFP1/ RGN Δ4, pIRES- AcGFP1/ RGN Δ4,5 and pIRES- AcGFP1 empty vector were transfected into the cells using Fugene®6 Transfection Reagent (Roche) according to the manufacturer´s instructions. Fugene®6 Reagent was diluted with serum-free medium (without antibiotics or fungicides), mixed and incubated during 5min. The plasmid DNA was added to the diluted Fugene 6 Transfection Reagent, mixed and incubated 25min at RT. For all cells were tested different Fugene 6 Transfection Reagent: µg DNA ratios to optimize transfection experiments (Table 6) The complex was added to the cells and 7 hours after medium was replaced with fresh medium containing antibiotic and FBS. After 48h and 72h, lamellas with transfected (pIRES-AcGFP1/RGN or pIRES-AcGFP1 alone) and non-transfected cells (negative control) were fixed with PFA 4% (pH=7,4), incubated with hoechst solution (Invitrogen) which labels cells nuclei, and mounted with Fluorescence Mounting Medium (Dako).

Finally, mounted cells were visualized in a fluorescence microscope (ZEISS) using the AxioVision software.

Table 6: Ratios tested in transient transfection experiments of PC3, LnCAP, PNT1A and PNT2 with pIRES-AcGFP1/RGNwt, pIRES- AcGFP1/RGN Δ4, pIRES- AcGFP1/ RGN Δ4,5 and pIRES- AcGFP1 vectors in a 24 well plate.

Ratio	3:1	3:2
SFM (µl)	19,4	19,4
Fugene 6 reagent (µl)	0,6	0,6
Vector DNA (µg)	0,2	0,4

9. Quantitative Polymerase Chain Reaction (q.PCR)

Quantitative PCR was performed to investigate the mRNA expression levels of RGN in prostate tissue of rats with different ages: 20 days, 1, 3, 6, 8 and 12 M.

For amplification of rat RGN, specific primers were used resulting in a fragment of 137bp. To normalize the expression of RGN, rat β-Actin and rat GAPDH primers were used as internal controls (Table 7). For PCR, Maxima^{TM} SYBR Green/Fluorescein qPCR Master Mix (2x) was used and the reactions were carried out using 1µg of cDNA synthesized from rat prostate tissues in a 20µl reaction containing 10µl of SYBR Green Supermix (Biorad) and 500nM of RGN or 200nM of β-Actin or GAPDH primers. Conditions and reagents concentrations were previously optimized. Reaction conditions comprised a 5min denaturation at 95ºC, followed by 40 cycles at 95ºC for 10 seconds, 60ºC for 30 seconds and 72ºC for 10 seconds. The amplified PCR fragments were analyzed by melting curves. Samples were run in triplicate in each PCR assay. Fold differences were calculated following the mathematical model proposed by Pfaffl using the formula: $2^{-\Delta\Delta Ct}$ (Pfaffl, 2001).

Table 7: Primers sequences, amplicon size and cycling conditions used in qPCR analysis.

Primers	Sequence	Amplicon size (bp)
rRGN_164fw **rRGN_301rv**	5´GGAGGAGGCATCAAAGTG´ 5´CAATGGTGGCAACATAGC3´	137
rGAPDH_2314fw **rGAPDH_2491rv**	5´GTTCAACGGCACAGTCAA3´ 5´CTCAGCACCAGCATCACC3´	177
rβActin_1235fw **rβAcin_1314rv**	5´ATGGTGGGTATGATGCAG3´ 5´CAATGCCGTGTTCAATGG3´	79

10. Data analysis

The statistical significance of differences in mRNA expression among experimental groups was assessed by ANOVA, followed by the Tukey test. Data analysis was performed using GraphPad Prism version 5.00 for Windows, GraphPad Software, San Diego California USA. Significant differences were considered when $p<0,05$. All experimental data are shown as mean ± SEM.

IV. Results

1. Analysis of regucalcin expression in rat prostate tissues at different post-natal ages

The expression of RGN at post-natal ages (20 days, 1M, 2M, 3M, 4M, 6M, 8M and 12M) in prostate rat tissues was analyzed by qPCR and normalized with the expression of β- actin and GAPDH housekeeping genes (Table 7).

The expression of RGN in rat prostate shows an increase at 3M (~two-fold), which is maintained at 4M and 6M. At 8M, RGN expression is markedly reduced, situation which is maintained in 12M old animals (Figure 16).

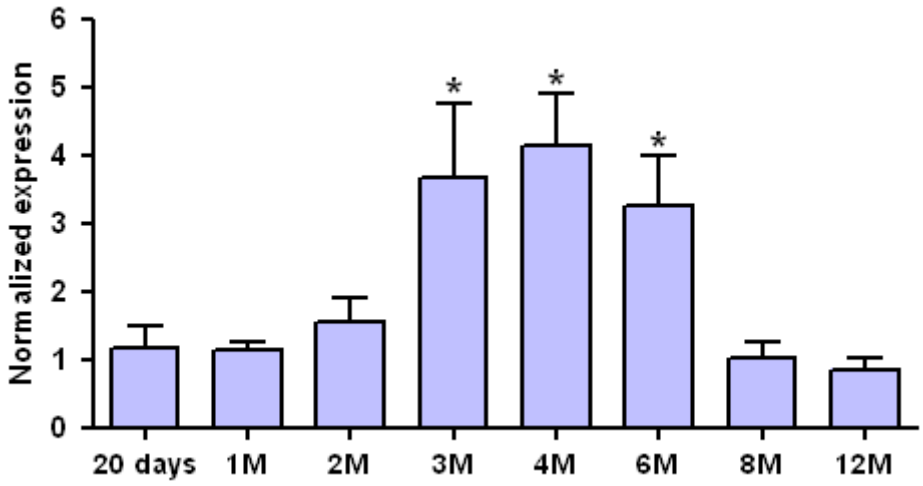

Figure 16: Expression of regucalcin (RGN) at different post-natal ages in prostate rat tissues determined by quantitative PCR (qPCR). RGN gene expression was normalized to β-Actin and GAPDH expression; * - Significantly different from other groups (P<0,05).

2. Expression of Regucalcin in human prostate cell lines and tissue-sections

The presence of RGN protein in human neoplasic and non-neoplasic prostate cell lines was determined by Western blot analysis which showed an immunoreactive band of approximately 35 kDa (Figure 17). A band with a lower molecular weight of ~30 kDa is also visible. Protein liver extract was used as a positive control.

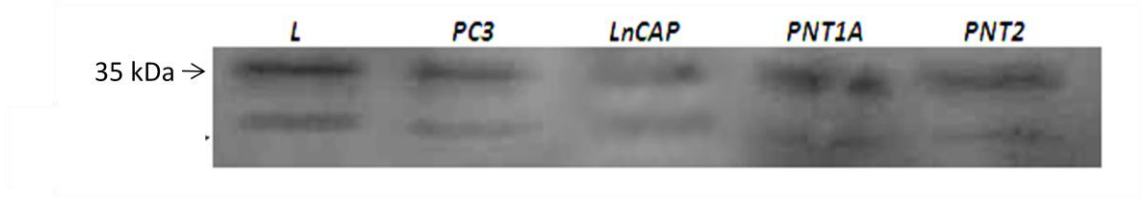

Figure 17: Western blot analysis of regucalcin in Human Prostate cancer (PC3 and LnCAP) and immortalized epithelial prostate (PNT1A and PNT2) cell lines using an anti-regucalcin monoclonal antibody (1:200); L- Liver, Positive control; Molecular weight is indicated in kDa on the left hand side.

The presence and cellular localization of RGN in human neoplasic prostate was analyzed by IHC (Figure 18). It was possible to confirm its expression in the tumor samples analyzed. RGN positive immunoreactivity was detected in cytoplasm (Figure 18) and nuclei (Figure 18 C and G) of prostate epithelial cells. It seems that panels E, G display a stronger staining for RGN comparatively with panels A, C, which correspond to a different tumor case.

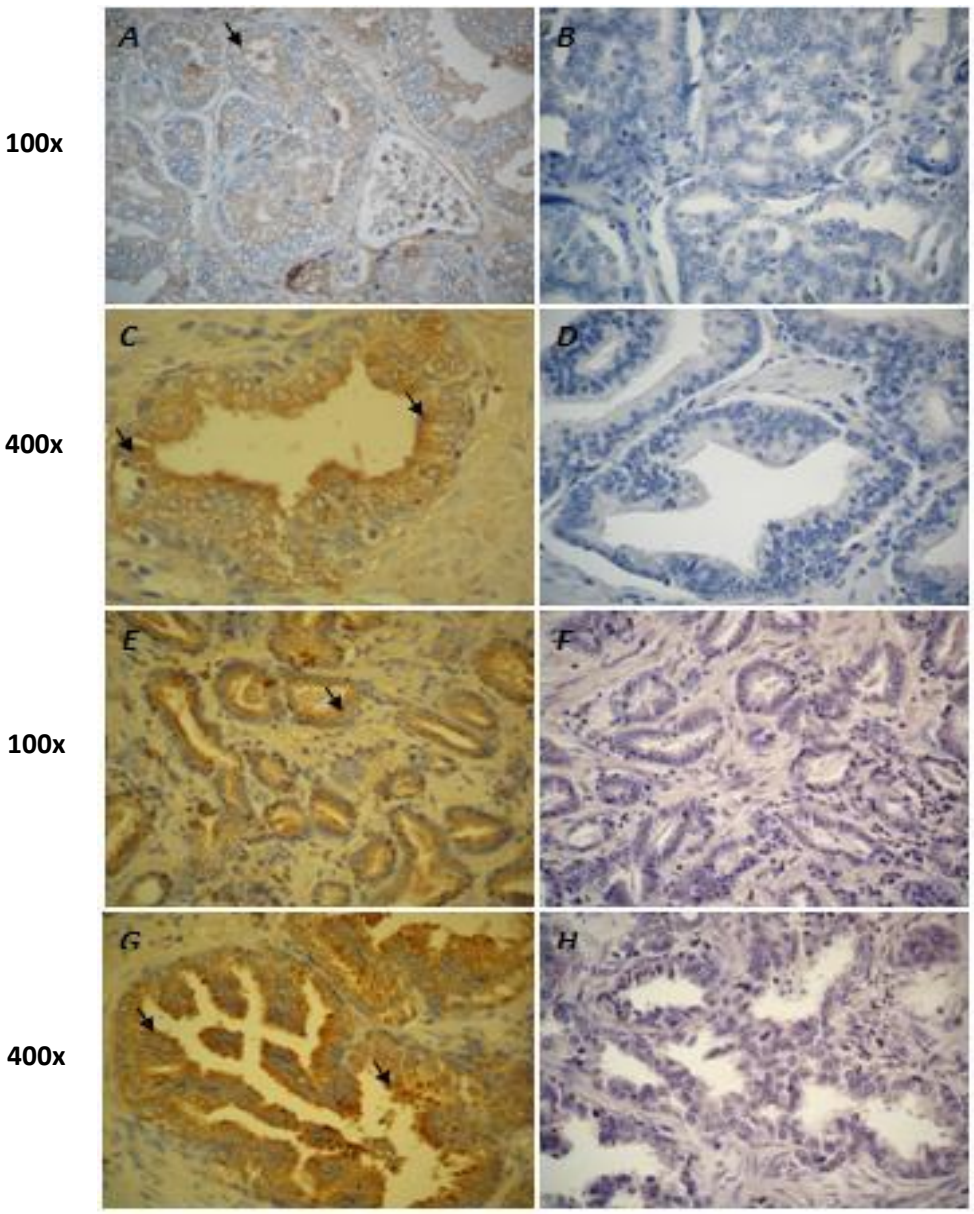

Figure 18: Regucalcin protein immunolocalization in human neoplasic prostate tissues. A, C, E, G Prostate carcinoma slides incubated with mouse monoclonal primary antibody anti-human Regucalcin (Abcam, ab81721) diluted 1:50, in an original magnification of 100x and 400x. The corresponding negative controls obtained by omission of primary antibody are shown in panels B, D, F and H. A, C and E, G correspond to two different cases.

3. Construction of Regucalcin expression vectors

The wt, Δ4 and Δ4,5 RGN transcripts were amplified by RT-PCR from human liver cDNA, cloned in pGEM-T easy vector and, after restriction digestion, subcloned in pIRES2-AcGFP1 vector.

The PCR reaction using a 5'-primer containing a NheI restriction site and a 3´-primer containing a XhoI restriction site (Table 3), allowed amplification of wt RGN and Δ4 and Δ4,5 transcript variants, with 897bp, 681bp and 549bp respectively (Figure 19 A). These PCR products, purified individually from an agarose gel, were cloned in pGEM-T easy vector. The sequence of all amplicons was determined to confirm identity and integrity before cloning in the expression vector. wt, Δ4 and Δ4,5 RGN cDNAs were isolated from pGEM-T easy vector by double-digestion with NheI and XhoI, gel purified and subcloned into the pIRES2-AcGFP1 expression vector which was previously digested with the same restriction enzymes.

The presence of wt, Δ4 and Δ4,5 RGN inserts in the expression vector was confirmed by digestion of the pIRES-AcGFP1/ RGN wt, Δ4 and Δ4,5 with EcoRI/NheI restriction enzymes (Figure 19 B).

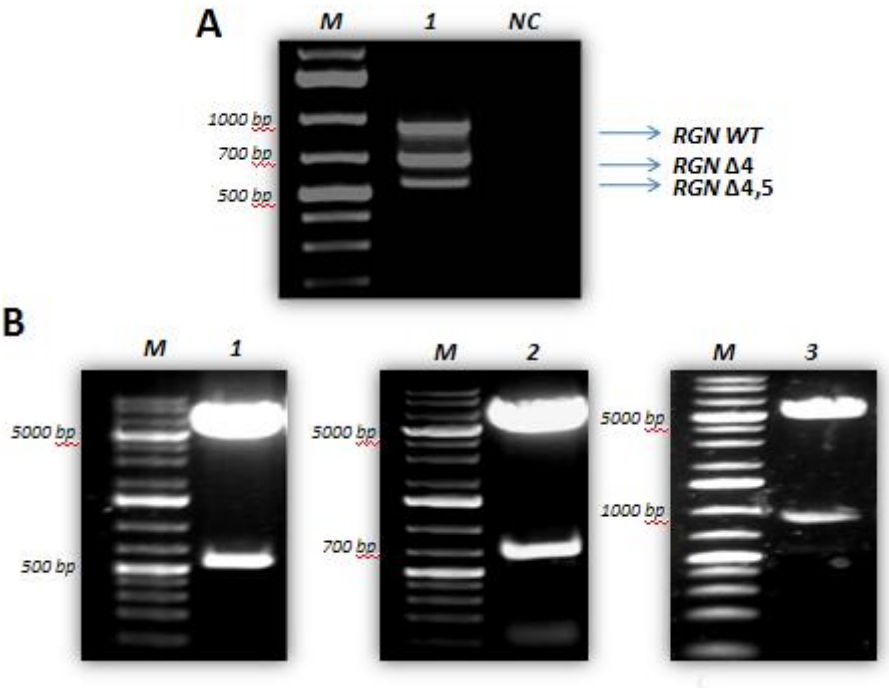

Figure 19: Cloning of wt and RGN transcription variants cDNAs in pIRES expression vector. **A**. RT-PCR amplification of wt RGN cDNA and Δ4, Δ4,5 alternative transcripts using specific primers with NheI/ XhoI restriction sites (1); NC- Negative control. **B**. RGNΔ4/pIRES (**1**), RGNΔ4,5/pIRES (**2**) and RGN wt/pIRES (**3**) plasmids digested with EcoRI/ Nhe1 . **M**- Molecular weight Marker (GeneRuler 1Kb Plus DNA Ladder).

4. RGN overexpression in neoplasic and non-neoplasic prostate cell lines

pIRES-AcGFP1/RGNwt, pIRES-AcGFP1/RGNΔ4 and pIRES-AcGFP1/RGNΔ 4,5 expression vectors were purified and used to transfect neoplasic (PC3 and LnCAP) and non-neoplasic (PNT1A and PNT2) prostate cell lines. After an appropriate growth period, we were able to detect transfected cells, and to localize RGN-GFP recombinant protein, by fluorescence microscopy. The cell nuclei were labeled with Hoechst solution and detected as blue.

.Transfection of PC3 and PNT1A prostate cells with pIRES-AcGFP1/ RGNwt and pIRES-AcGFP1 empty vectors was confirmed by immunofluorescence.

RGN transfection in PC3 (Figure 20) and PNT1A (Figure 21) cells was achieved 48h after transfection, using a 3:1 Fugene: µg DNA vector ratio. Co-localization of RGN and nucleus is shown in the merged figures (figure 20, panel I and figure 21, panel F), which confirms RGN transfection. PC3 cells transfected with the pIRES-AcGFP1 empty vector only display Hoescht or GFP fluorescence (figure 20, panels D, E and F).

Transfection experiments of PC3 and PNT1A cells with pIRES-AcGFP1/RGN Δ4 and pIRES- AcGFP1/RGN Δ4,5 expression vectors is underway.

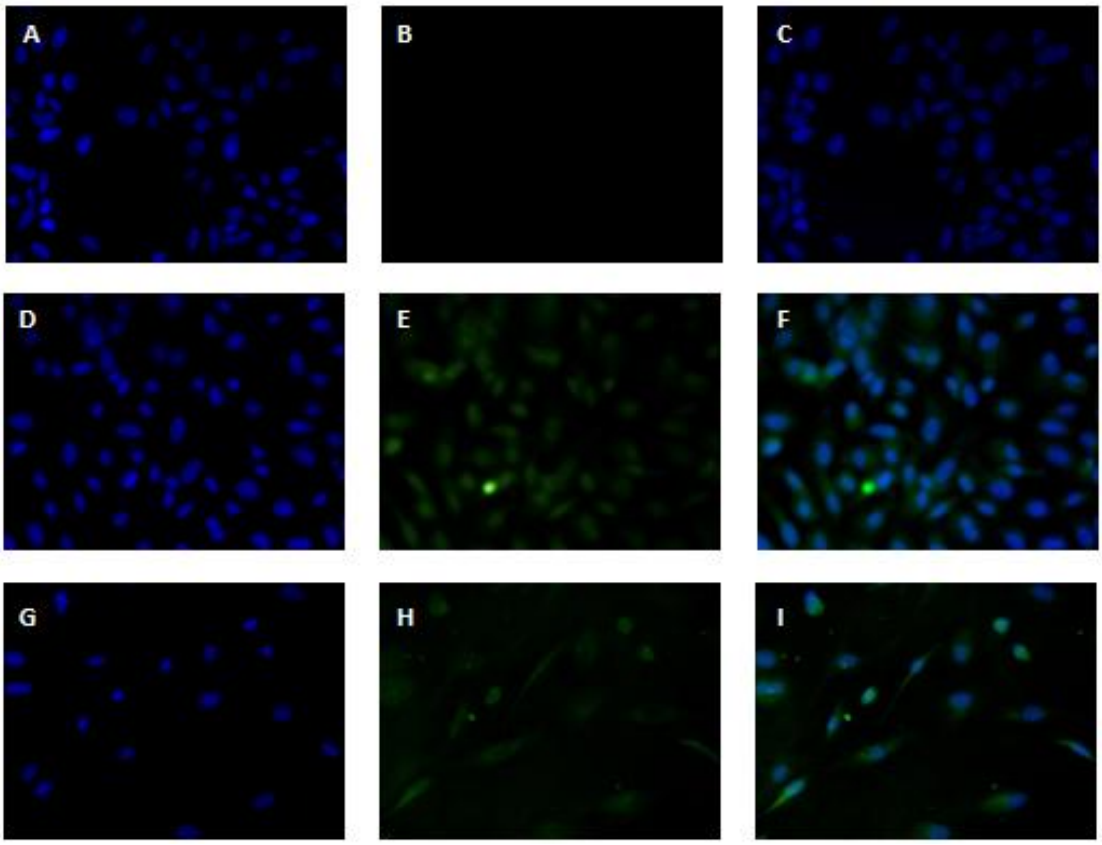

Figure 20: Dual fluorescence localization of RGN-GFP protein (green) and nucleus (blue) in PC3 cells. PC3 cells were transfected using a 3:1, Fugene:µg DNA vector ratio in transfection procedure and for 48h. A, B, C. Negative control without transfection reagent and DNA; D, E, F. PC3 cells transfected with pIRES- AcGFP1 empty vector; G, H, I. PC3 cells transfected with pIRES- AcGFP1/ RGNwt vector. Co-localization of RGN and nucleus is shown in the merged figure as light blue (I). All panels are shown in an original magnification of 400x.

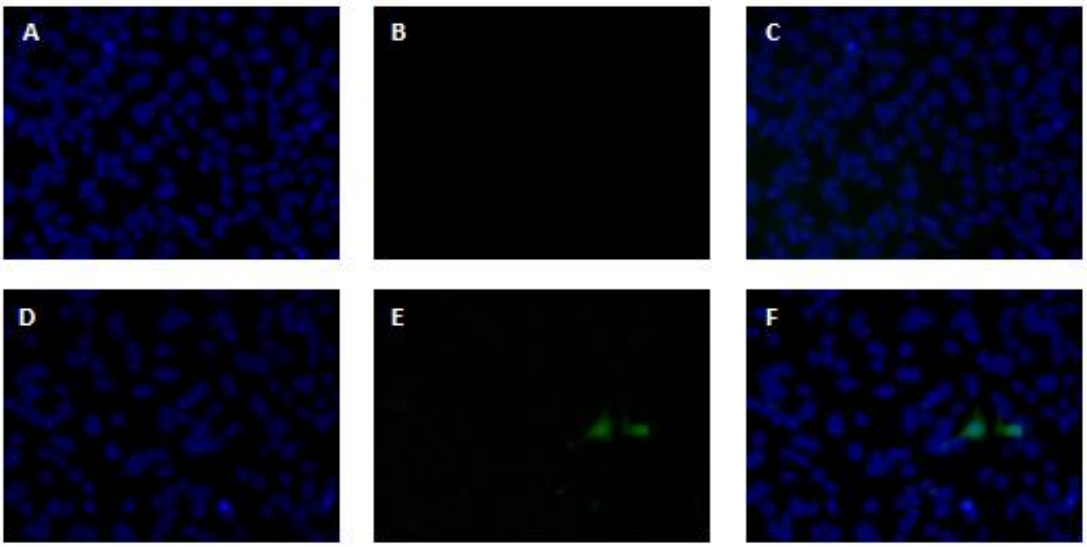

Figure 21: Dual fluorescence localization of RGN-GFP protein (green) and nucleus (blue) in PNT1A cells. PNT1A cells were transfected using a 3:1, Fugene:µg DNA vector ratio in transfection procedure and for 48h. A, B, C. Negative control without transfection reagent and DNA; D, E, F. PNT1A cells transfected with pIRES- AcGFP1/ RGNwt vector. Co-localization of RGN and nucleus is shown in the merged figure as light blue (F). All panels are shown in an original magnification of 400x.

5. Optimization of RT-PCR amplification of oncogenes and tumor suppressor genes in prostate cell lines

The expression of oncogenes (BCL2, Ha-ras and c-myc) and TSGs (p53 and RB1) was evaluated by RT-PCR analysis in neoplasic (PC3, LnCAP) and non-neoplasic (PNT1A and PNT2) prostate cell lines (Figure 22) using specific primer sets (Table 2). 18S was amplified in order to normalize cDNA loading in each PCR reaction and to determine relative expression ratios of oncogenes and TSGs in neoplasic and non-neoplasic cell lines (Figure 23).

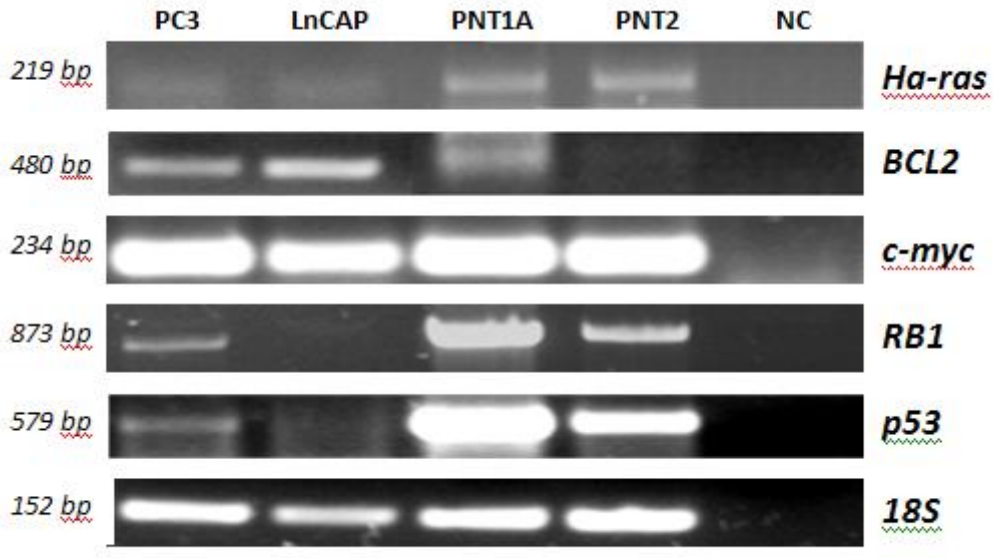

Figure 22: Expression of oncogenes (BCL2, Ha-ras and c-myc) and tumor supressor genes (p53 and RB1) in Human Prostate cancer (PC3 and LnCAP) and immortalized epithelial prostate (PNT1A and PNT2) cell lines determined by RT-PCR using specific primers. 18S amplification was used to normalize cDNA loading in each reaction and to determine relative expression ratios of oncogenes and tumor suppressor genes; NC- Negative control (no cDNA added); Molecular weight is indicated in bp on the left hand side.

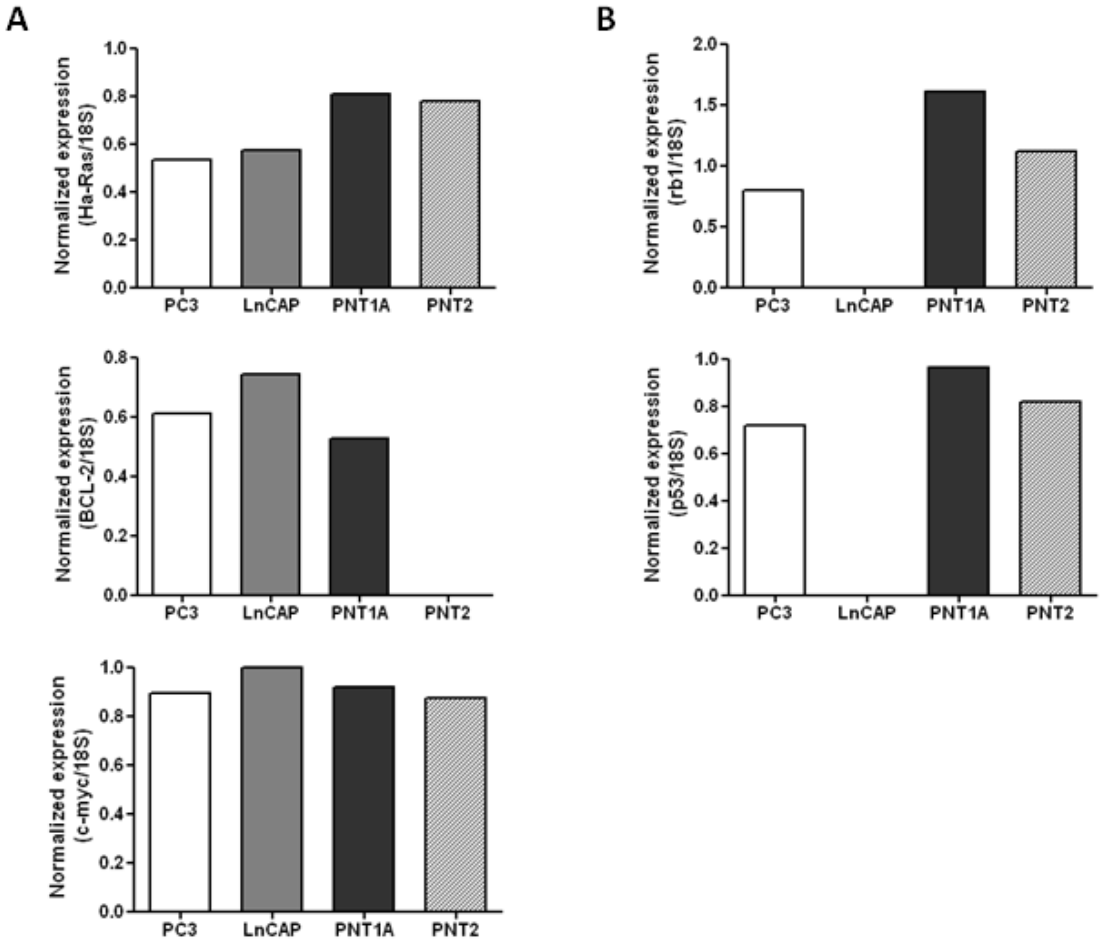

Figure 23: Normalized expression of oncogenes (A) (BCL2, Ha-ras and c-myc) and tumor suppressor genes (B) (p53 and RB1) in Human Prostate cancer (PC3 and LnCAP) and immortalized epithelial prostate (PNT1A and PNT2) cell lines determined by RT-PCR. The semi-quantitative expression of the studied genes was determined using Bio-1D v99.04 program and normalized with the expression of 18S in the different cell lines analyzed.

The oncogene, c-myc, is highly expressed in all prostate cell lines analysed. Ha-ras is detected in all cell lines, but exhibited variable levels of expression. It is most expressed in the immortalized epithelial prostate cell lines (PNT1A and PNT2). BCL2 is predominantly expressed in the neoplasic (PC3 and LnCAP) cell lines.

Both TSGs, RB1 and p53, are abundantly expressed in non-neoplasic prostate cell lines (PNT1A and PNT2) contrastingly with the neoplasic cells.

V. Discussion

RGN, also now as SMP30, is involved in maintenance of Ca^{2+} homeostasis due to the activation of Ca^{2+} pumping enzymes in the plasma membrane (Yamaguchi, 2000a). It has a suppressive effect in cell proliferation, DNA and RNA synthesis, and may be associated with the abnormal cell division on tumor tissues (Tsurusaki et al., 2000).

Fujita et al (1996) described the expression of RGN in livers and kidneys of rats from the embryonic to the senescent stages of life. RGN decrease with aging in the livers of rats, showing a marked increase in livers of neonatal and young rats and a down-regulation with age (Fujita et al., 1996a). Recently our research group identified the presence of RGN in prostate (Maia et al., 2008).

In the present study, using qPCR analysis, we determined the expression of RGN in rat prostate at different post-natal ages. The RGN gene expression showed a significant increase at 3M, maintaining that expression level in 4M and 6M old adults. In the adult, the prostate gland size is maintained through a homeostatic balance between the process of renewal (proliferation) and cell death (apoptosis). This balance is regulated by hormones secreted by the endocrine system, mainly androgens (Prins et al., 1996, Shibata et al., 2000). It has been show that RGN regulates proliferation and apoptosis processes (Tsurusaki and Yamaguchi, 2003a, Nakagawa and Yamaguchi, 2005, Yamaguchi and Daimon, 2005) and our previous results demonstrated that its expression is up-regulated by androgens (*unpublished results*) which likely justifies the observed increase of expression in adult rats. In 8M and 12M old rats prostate RGN expression is diminished, which is in accordance with the expression pattern described in the liver and kidney, referring RGN as a senescence protein (Fujita et al., 1996a). These results revealed that RGN is developmentally regulated in prostate tissue and suggested their requirement for maintaining tissue specific functions.

Recently, our research group identified RGN mRNA and protein in neoplasic and non-neoplasic prostate tissues and LnCAP cells (Maia et al., 2008, Maia et al., 2009). In this report, we confirmed the expression of RGN protein in neoplasic and non-neoplasic prostate cell lines by western Blot and in human prostate cancer tissues by IHC. Western blot analysis using an anti-RGN monoclonal antibody showed an immunoreactive protein of approximately 35 kDa in LnCAP, PC3, PNT1A and PNT2A cells, which corresponds to the RGN predicted size, also previously reported by Fujita (1992).

In terms of RGN mRNA, a wt wild-type transcript and two transcript variants (Δ4 and Δ4,5) were identified in human breast and prostate tissue and cells. The Δ4 and Δ4,5 transcripts can be the result of alternative splicing events (Maia et al., 2009). It is not known at the moment if these transcripts are translated to proteins, however, the

immunoreactive protein with a molecular weight of ~30 kDa, may correspond to the protein encoded by the Δ4 transcript. Further studies are necessary to determine the *in vivo* presence and function of these hypothetical proteins. At least for our knowledge this is the first report describing RGN expression in PC3, PNT1A and PNT2 cells, demonstrating that these cell lines may also be useful models to study RGN actions in prostate patophysiology.

IHC analysis showed RGN immunoreactivity in human neoplasic prostate tissues with the protein being localized in the cytosol and nuclei of epithelial cells. One of the cases analyzed seems to display stronger staining for RGN, probably corresponding to a more advanced stage of cancer development since RGN immunoreactivity was associated with grade of cellular differentiation of prostate adenocarcinoma (Maia et al., 2009). This finding suggests that RGN may have a protective role against prostate carcinogenesis. In the future, it is important to understand which are the factors involved in the control of RGN expression.

Prostate cell lines were transfected with pIRES-AcGFP1/ RGNwt and, pIRES-AcGFP1 empty vectors. The successful transfection of PC3 and PNT1A cells was confirmed by the presence of RGN-GFP protein in cells nuclei and cytoplasm. These results are concordant with the described IHC localization of RGN. RGN has been shown to translocate into the nucleus of rat liver (Tsurusaki et al., 2000), and the protein has an inhibitory effect on RNA synthesis in isolated rat liver nucleus (Tsurusaki and Yamaguchi, 2002). It is speculated that RGN may bind to promoter region of tumor-related genes and that the protein may suppress the expression of tumor stimulator gene and stimulate the expression of TSG in the cloned rat hepatoma H4-II-E cells overexpressing RGN. It is speculated that RGN may partly inhibit the action of intracellular signaling factors that are related to gene expression (Tsurusaki and Yamaguchi, 2003a). Considering the cellular effects ascribed to RGN, the demonstration of its presence and cellular localization in neoplasic prostate tissues and the localization of the protein RGN-GFP in transfected PC3 and PNT1A cells, it is liable to speculate that this protein translocates into the nucleus and it modulates gene expression.

The disequilibrium in cell death and proliferation is on the basis of carcinogenesis, and the malignant transformation of cells has been associated with alterations in Ca^{2+} signaling (Prevarskaya et al., 2004). RGN seems to have dual effect in suppression of the cells proliferation and apoptosis stimulation. The suppressive effect of RGN on cell proliferation is related to its inhibitory effect on the activities of various protein kinases and protein phosphatases, Ca^{2+}- dependent signaling factors, nuclear DNA, RNA, and protein synthesis or IGF-I expression, and its activatory effect

on p21, an inhibitor of cell cycle-related protein kinases (Tsurusaki and Yamaguchi, 2003a). Overexpression of RGN has been shown to have a suppressive effect on cell death and apoptosis induced by TNF-α, LPS, Bay K 8644, or thapsigargin, which induces apoptotic cell death mediated by various intracellular signaling. It is speculated that RGN plays a role in the regulation of BCL2 gene expression, a suppressor in apoptotic cell death (Izumi and Yamaguchi, 2004). PC is an endocrine cancer which depends on the trophic effects of estrogens and androgens, and altered Ca^{2+} homeostasis and signaling have been associated with the development of this pathology (Prevarskaya et al., 2004, Maia et al., 2009). RGN expression was identified in prostate neoplasic tissues (Maia et al., 2009).

RGN suppresses cell proliferation (Nakagawa and Yamaguchi, 2005, Yamaguchi and Daimon, 2005), inhibits expression of oncogenes c-myc, H-ras, and c-src, and increases the expression of tumour supressor genes p53 and Rb (Tsurusaki and Yamaguchi, 2003a, Tsurusaki and Yamaguchi, 2004). In this work, we optimized the RT- PCR amplification of oncogenes and TSGs primers in PC3, LnCAP, PNT1A and PNT1A2 cells, in order to pursue to additional studies upon RGN overexpression in these cell lines. As expected, highly expression of both TSGs, RB1 and p53, was observed in non-neoplasic prostate cell lines (PNT1A and PNT2) contrastingly with the neoplasic cells. Oncogenes are differentially expressed in the different cell lines, which may represent a proper specific gene expression of each cell line.

From the previous and the present observations, we can assume that deregulation of RGN function may have a relevant role in prostate cancer initiation and/or progression, and the presence of the RGN-GFP in the nucleus of PC3 and PNT1A transfected cells suggests a possible influence of RGN in the expression of oncogenes and TSGs in the prostate cell lines overexpressing RGN. To achieve this goal the transfection efficiency of all cell lines with pIRES-constructed vectors will be optimized. Overexpression will be confirmed by means of Western Blot. It is expected a suppression of oncogenes and stimulation of TSGs achieved by RGN overexpression after transfection with pIRES-AcGFP1/ RGNwt vector.

The RGN protein is a molecule with hydrophilic character. This hydrophilic region, which has been suggested as the functional domain related to Ca^{2+} binding [Shimokawa and Yamaguchi, 1993b], is deleted in the putative proteins originated from the Δ4 and Δ4,5 transcript. Ca^{2+} binding was suggested to occur also by involvement of aspartic acid and glutamine residues (Yamaguchi, 2000a) and the putative proteins generated from RGN transcript variants may have loss up to 52% of glutamine and aspartic acid residues (Maia et al., 2009). Thus, it is liable to speculate that these proteins may lack the ability for Ca^{2+} binding. The alteration of splicing patterns of

several genes has been associated with cancer, and these alternative transcripts can be associated to alternative splicing. Δ4 and Δ4,5 RGN transcripts mRNA expression indicate a relevant physiological role in normal and pathologic physiology (Maia et al., 2009). Cells transfection with pIRES-AcGFP1/ RGNΔ4 and pIRES-AcGFP1/ RGNΔ4,5 vectors will allow to understand if RGN transcripts are translated to protein, display the same cellular localization of wt RGN and maintain the RGN roles in cell proliferation and gene expression.

VI. References

ABATE-SHEN, C. & SHEN, M. (2002) Mouse models of prostate carcinogenesis. *Trends in Genetics,* 18**,** S1-S5.

ABEELE, F., SHUBA, Y., ROUDBARAKI, M., LEMONNIER, L., VANOVERBERGHE, K., MARIOT, P., SKRYMA, R. & PREVARSKAYA, N. (2003) Store-operated Ca2+ channels in prostate cancer epithelial cells: function, regulation, and role in carcinogenesis. *Cell Calcium,* 33**,** 357-373.

ABEELE, F., SKRYMA, R., SHUBA, Y., VAN COPPENOLLE, F., SLOMIANNY, C., ROUDBARAKI, M., MAUROY, B., WUYTACK, F. & PREVARSKAYA, N. (2002) Bcl-2-dependent modulation of Ca2+ homeostasis and store-operated channels in prostate cancer cells. *Cancer Cell,* 1**,** 169-179.

BRADFORD, M. (1976) A rapid and sensitive method for the quantitation of microgram quantities of protein utilizing the principle of protein-dye binding. *Analytical biochemistry,* 72**,** 248-254.

CARAFOLI, E. (1987) Intracellular calcium homeostasis. *Annual Review of Biochemistry,* 56**,** 395-433.

CHAKRABORTI, S. & BAHNSON, B. (2010) Crystal Structure of Human Senescence Marker Protein 30; Insights Linking Structural, Enzymatic and Physiological Functions. *Biochemistry,* 49**,** 3436–3444

DE MARZO, A., NAKAI, Y. & NELSON, W. (2007) Inflammation, atrophy, and prostate carcinogenesis. Elsevier.

DING, Y., ROBBINS, J., FRASER, S., GRIMES, J. & DJAMGOZ, M. (2006) Comparative studies of intracellular Ca2+ in strongly and weakly metastatic rat prostate cancer cell lines. *International Journal of Biochemistry and Cell Biology,* 38**,** 366-375.

FUJITA, T. (1999) Senescence marker protein-30 (SMP30): structure and biological function. *Biochem Biophys Res Commun,* 254**,** 1-4.

FUJITA, T., MANDEL, J., SHIRASAWA, T., HINO, O., SHIRAI, T. & MARUYAMA, N. (1995) Isolation of cDNA clone encoding human homologue of senescence marker protein-30 (SMP30) and its location on the X chromosome. *BBA-Gene Structure and Expression,* 1263**,** 249-252.

FUJITA, T., SHIRASAWA, T. & MARUYAMA, N. (1996a) Isolation and characterization of genomic and cDNA clones encoding mouse senescence marker protein-30 (SMP30). *BBA-Gene Structure and Expression,* 1308**,** 49-57.

FUJITA, T., SHIRASAWA, T., UCHIDA, K. & MARUYAMA, N. (1992) Isolation of cDNA clone encoding rat senescence marker protein-30 (SMP30) and its tissue distribution. *Biochimica et biophysica acta,* 1132**,** 297.

FUJITA, T., SHIRASAWA, T., UCHIDA, K. & MARUYAMA, N. (1996b) Gene regulation of senescence marker protein-30 (SMP30): coordinated up-regulation with tissue maturation and gradual down-regulation with aging. *Mechanisms of ageing and development,* 87**,** 219-229.

GRAAFF, V. (2002) Human anatomy, McGraw-Hill.

ISHIGAMI, A., FUJITA, T., HANDA, S., SHIRASAWA, T., KOSEKI, H., KITAMURA, T., ENOMOTO, N., SATO, N., SHIMOSAWA, T. & MARUYAMA, N. (2002) Senescence Marker Protein-30 Knockout Mouse Liver Is Highly Susceptible to Tumor Necrosis Factor-{alpha}-and Fas-Mediated Apoptosis. *American Journal of Pathology,* 161**,** 1273.

IZUMI, T. & YAMAGUCHI, M. (2004) Overexpression of regucalcin suppresses cell death and apoptosis in cloned rat hepatoma H4-II-E cells induced by lipopolysaccharide, PD 98059, dibucaine, or Bay K 8644. *Journal of Cellular Biochemistry,* 93**,** 598-608.

JIN-RONG, Z., LUNYIN, Y., LUIZ, F., TOWIA, A. & GEORGE, L. (2004) Progression to androgen-independent LNCaP human prostate tumors: cellular and molecular alterations. *International journal of cancer. Journal international du cancer,* 110**,** 800.

JOSHUA, A., EVANS, A., VAN DER KWAST, T., ZIELENSKA, M., MEEKER, A., CHINNAIYAN, A. & SQUIRE, J. (2008) Prostatic preneoplasia and beyond. *BBA-Reviews on Cancer,* 1785**,** 156-181.

KNOBIL, E. & NEILL, J. (2006) *Knobil and Neill's physiology of reproduction*, Academic Press.

KONDO, Y., INAI, Y., SATO, Y., HANDA, S., KUBO, S., SHIMOKADO, K., GOTO, S., NISHIKIMI, M., MARUYAMA, N. & ISHIGAMI, A. (2006) Senescence marker protein 30 functions as gluconolactonase in L-ascorbic acid biosynthesis, and its knockout mice are prone to scurvy. National Acad Sciences.

KONDO, Y., ISHIGAMI, A., KUBO, S., HANDA, S., GOMI, K., HIROKAWA, K., KAJIYAMA, N., CHIBA, T., SHIMOKADO, K. & MARUYAMA, N. (2004) Senescence marker protein-30 is a unique enzyme that hydrolyzes diisopropyl phosphorofluoridate in the liver. *FEBS letters,* 570**,** 57-62.

KUROTA, H. & YAMAGUCHI, M. (1997) Inhibitory effect of regucalcin on Ca 2+/calmodulin-dependent protein kinase activity in rat renal cortex cytosol. *Molecular and cellular biochemistry,* 177**,** 239-243.

KUROTA, H. & YAMAGUCHI, M. (1998) Inhibitory effect of calcium-binding protein regucalcin on protein kinase C activity in rat renal cortex cytosol. *Biological & pharmaceutical bulletin,* 21**,** 315.

LOPEZ-OTIN, C. & DIAMANDIS, E. (1998) Breast and prostate cancer: an analysis of common epidemiological, genetic, and biochemical features. *Endocrine reviews,* 19**,** 365-396.

MAIA, C., SANTOS, C., SCHMITT, F. & SOCORRO, S. (2008) Regucalcin is expressed in rat mammary gland and prostate and down-regulated by 17 -estradiol. *Molecular and cellular biochemistry,* 311**,** 81-86.

MAIA, C., SANTOS, C., SCHMITT, F. & SOCORRO, S. (2009) Regucalcin is under-expressed in human breast and prostate cancers: Effect of sex steroid hormones. *Journal of Cellular Biochemistry,* 107.

MARUYAMA, N., ISHIGAMI, A. & KONDO, Y. (2010) Pathophysiological significance of senescence marker protein-30. *Geriatrics & Gerontology International,* 10**,** S88-S98.

MATSUYAMA, S., KITAMURA, T., ENOMOTO, N., FUJITA, T., ISHIGAMI, A., HANDA, S., MARUYAMA, N., ZHENG, D., IKEJIMA, K. & TAKEI, Y. (2004) Senescence marker protein-30 regulates Akt activity and contributes to cell survival in Hep G2 cells. *Biochemical and Biophysical Research Communications,* 321**,** 386-390.

MCNEAL, J. (1980) The anatomic heterogeneity of the prostate. *Progress in clinical and biological research,* 37**,** 149.

MCNEAL, J. (1988) Normal histology of the prostate. *The American journal of surgical pathology,* 12**,** 619.

MCNEAL, J. (2006) Anatomy of the prostate: an historical survey of divergent views. *The prostate,* 1**,** 3-13.

MCNEAL, J., REDWINE, E., FREIHA, F. & STAMEY, T. (1988) Zonal distribution of prostatic adenocarcinoma: correlation with histologic pattern and direction of spread. *The American journal of surgical pathology,* 12**,** 897.

MEYER, H., AHRENS-FATH, I., SOMMER, A. & HAENDLER, B. (2004) Novel molecular aspects of prostate carcinogenesis. *Biomedecine & Pharmacotherapy,* 58**,** 10-16.

MIMEAULT, M. & BATRA, S. (2006) Recent advances on multiple tumorigenic cascades involved in prostatic cancer progression and targeting therapies. *Carcinogenesis,* 27**,** 1.

MISAWA, H., INAGAKI, S. & YAMAGUCHI, M. (2002) Suppression of cell proliferation and deoxyribonucleic acid synthesis in cloned rat hepatoma H4-II-E cells overexpressing regucalcin. *Journal of Cellular Biochemistry,* 84**,** 143-149.

NAKAGAWA, T. & YAMAGUCHI, M. (2005) Overexpression of regucalcin suppresses apoptotic cell death in cloned normal rat kidney proximal tubular epithelial NRK52E cells: Change in apoptosis-related gene expression. *Journal of Cellular Biochemistry,* 96**,** 1274-1285.

NAKAGAWA, T. & YAMAGUCHI, M. (2006) Overexpression of regucalcin enhances its nuclear localization and suppresses L-type Ca2+ channel and calcium-sensing receptor mRNA expressions in cloned normal rat kidney proximal tubular epithelial NRK52E cells. *Journal of Cellular Biochemistry,* 99**,** 1064-1077.

NETTER, F. (1997) Atlas of human anatomy. ICON Learning Systems, LLC. 167.

PFAFFL, M. (2001) A new mathematical model for relative quantification in real-time RT-PCR. *Nucleic acids research,* 29**,** e45.

PONDER, B. (2001) Cancer genetics. *Nature,* 411**,** 336-341.

PREVARSKAYA, N., SKRYMA, R. & SHUBA, Y. (2004) Ca2+ homeostasis in apoptotic resistance of prostate cancer cells. *Biochemical and Biophysical Research Communications,* 322**,** 1326-1335.

PRINS, G., JUNG, M., VELLANOWETH, R., CHATTERJEE, B. & ROY, A. (1996) Age-dependent expression of the androgen receptor gene in the prostate and its implication in glandular differentiation and hyperplasia. *Developmental genetics,* 18**,** 99-106.

RAMSAY, A. & LEUNG, H. (2009) Signalling pathways in prostate carcinogenesis: potentials for molecular-targeted therapy. *Clinical science (London, England: 1979),* 117**,** 209.

SCHULZ, W. & HOFFMANN, M. (2009) Epigenetic mechanisms in the biology of prostate cancer. Elsevier.

SCIARRA, A., MARIOTTI, G., SALCICCIA, S., GOMEZ, A., MONTI, S., TOSCANO, V. & DI SILVERIO, F. (2008) Prostate growth and inflammation. *Journal of Steroid Biochemistry and Molecular Biology,* 108**,** 254-260.

SHAPIRO, E., HUANG, H., MASCH, R., MCFADDEN, D., WILSON, E. & WU, X. (2005) Immunolocalization of estrogen recepor [alpha] and [beta] in human fetal prostate. *The Journal of urology,* 174**,** 2051-2053.

SHIBATA, Y., ITO, K., SUZUKI, K., NAKANO, K., FUKABORI, Y., SUZUKI, R., KAWABE, Y., HONMA, S. & YAMANAKA, H. (2000) Changes in the endocrine environment of the human prostate transition zone with aging: simultaneous quantitative analysis of prostatic sex steroids and comparison with human prostatic histological composition. *The prostate,* 42**,** 45-55.

SHIMOKAWA, N. & YAMAGUCHI, M. (1993) Molecular cloning and sequencing of the cDNA coding for a calcium-binding protein regucalcin from rat liver. *FEBS letters,* 327**,** 251.

TAKAHASHI, H. & YAMAGUCHI, M. (1994) Activating effect of regucalcin on (Ca 2+-Mg 2+)-ATPase in rat liver plasma membranes: relation to sulfhydryl group. *Molecular and cellular biochemistry,* 136**,** 71-76.

TAKAHASHI, H. & YAMAGUCHI, M. (1999) Role of regucalcin as an activator of Ca 2 ATPase activity in rat liver microsomes. *Journal of Cellular Biochemistry,* 74**,** 663-669.

TAKAHASI, H. & YAMAGUCHI, M. (1996) Enhancement of plasma membrane (Ca 2+-Mg 2+)-ATPase activity in regenerating rat liver: Involvement of endogenous activating protein regucalcin. *Molecular and cellular biochemistry,* 162**,** 133-138.

TSURUSAKI, Y., MISAWA, H. & YAMAGUCHI, M. (2000) Translocation of regucalcin to rat liver nucleus: involvement of nuclear protein kinase and protein phosphatase regulation. *International journal of molecular medicine,* 6**,** 655.

TSURUSAKI, Y. & YAMAGUCHI, M. (2000) Role of endogenous regucalcin in the regulation of Ca 2-ATPase activity in rat liver nuclei. *Journal of Cellular Biochemistry,* 78**,** 541-549.

TSURUSAKI, Y. & YAMAGUCHI, M. (2002) Suppressive role of endogenous regucalcin in the enhancement of deoxyribonucleic acid synthesis activity in the nucleus of regenerating rat liver. *Journal of Cellular Biochemistry,* 85**,** 516-522.

TSURUSAKI, Y. & YAMAGUCHI, M. (2003a) Overexpression of regucalcin modulates tumor-related gene expression in cloned rat hepatoma H4-II-E cells. *Journal of Cellular Biochemistry,* 90**,** 619-626.

TSURUSAKI, Y. & YAMAGUCHI, M. (2003b) Role of endogenous regucalcin in transgenic rats: Suppression of protein tyrosine phosphatase and ribonucleic acid synthesis activities in liver nucleus. *International journal of molecular medicine,* 12**,** 207-211.

TSURUSAKI, Y. & YAMAGUCHI, M. (2004) Role of regucalcin in liver nuclear function: Binding of regucalcin to nuclear protein or DNA and modulation of tumor-related gene expression. *International journal of molecular medicine,* 14**,** 277-281.

VANOVERBERGHE, K., MARIOT, P., VANDEN ABEELE, F., DELCOURT, P., PARYS, J. & PREVARSKAYA, N. (2003) Mechanisms of ATP-induced calcium signaling and growth arrest in human prostate cancer cells. *Cell Calcium,* 34**,** 75-85.

YAMAGUCHI, M. (2000a) Role of regucalcin in calcium signaling. *Life sciences,* 66**,** 1769-1780.

YAMAGUCHI, M. (2000b) The role of regucalcin in nuclear regulation of regenerating liver. *Biochemical and Biophysical Research Communications,* 276**,** 1-6.

YAMAGUCHI, M. (2005) Role of regucalcin in maintaining cell homeostasis and function(Review). *International journal of molecular medicine,* 15**,** 371-389.

YAMAGUCHI, M. & DAIMON, Y. (2005) Overexpression of regucalcin suppresses cell proliferation in cloned rat hepatoma H4-II-E cells: Involvement of intracellular signaling factors and cell cycle-related genes. *Journal of Cellular Biochemistry,* 95**,** 1169-1177.

YAMAGUCHI, M. & KANAYAMA, Y. (1995) Enhanced expression of calcium-binding protein regucalcin mRNA in regenerating rat liver. *Journal of Cellular Biochemistry,* 57**,** 185-190.

YAMAGUCHI, M. & KUROTA, H. (1997) Inhibitory effect of regucalcin on Ca 2+/calmodulin-dependent cyclic AMP phosphodiesterase activity in rat kidney cytosol. *Molecular and cellular biochemistry,* 177**,** 209-214.

YAMAGUCHI, M., MOROOKA, Y., MISAWA, H., TSURUSAKI, Y. & NAKAJIMA, R. (2002) Role of endogenous regucalcin in transgenic rats: Suppression of kidney cortex cytosolic protein phosphatase activity and enhancement of heart muscle microsomal Ca2+-ATPase activity. *Journal of Cellular Biochemistry,* 86**,** 520-529.

YAMAGUCHI, M. & NISHINA, N. (1995) Characterization of regucalcin effect on proteolytic activity in rat liver cytosol: relation to cysteinyl-proteases. *Molecular and cellular biochemistry,* 148**,** 67-72.

YAMAGUCHI, M. & TAI, H. (1991) Inhibitory effect of calcium-binding protein regucalcin on Ca 2+/calmodulin-dependent cyclic nucleotide phosphodiesterase activity in rat liver cytosol. *Molecular and cellular biochemistry,* 106**,** 25-30.

YAMAGUCHI, M., TAKAKURA, Y. & NAKAGAWA, T. (2008) Regucalcin increases Ca2+-ATPase activity in the mitochondria of brain tissues of normal and transgenic rats. *Journal of Cellular Biochemistry,* 104**,** 795-804.

YAMAGUCHI, M. & YAMAMOTO, T. (1978) Purification of calcium binding substance from soluble fraction of normal rat liver. *Chemical & pharmaceutical bulletin,* 26**,** 1915.

YOUNG, B., AND HEATH, J. (2002) Functional histology. Churchill Livingstone.

VII. Attachments

Sequence analysis of RGN wt, Δ4 and Δ4,5 transcript variants after cloning and sequencing using NCBI's BLASTN software (www.ncbi.nlm.nih.gov, 2010) showed alignment with the mRNA and protein of RGN Homosapiens.

```
CLUSTAL 2.0.12 multiple sequence alignment


RGNWT1                  ----------------------------------------------------MDAPVSS 7
HomosapiensNM_004683    MSSIKIECVLPENCRCGESPVWEEVSNSLLFVDIPAKKVCRWDSFTKQVQRVTMDAPVSS 60
                                                                       *******

RGNWT1                  VALRQSGGYVATIGTKFCALNWKEQSAVVLATVDNDKKNNRFNDGKVDPAGRYFAGTMAE 67
HomosapiensNM_004683    VALRQSGGYVATIGTKFCALNWKEQSAVVLATVDNDKKNNRFNDGKVDPAGRYFAGTMAE 120
                        ************************************************************

RGNWT1                  ETAPAVLERHQGALYSLFPDHHVKKYFDQVDISNGLDWSLDHKIFYYIDSLSYSVDAFDY 127
HomosapiensNM_004683    ETAPAVLERHQGALYSLFPDHHVKKYFDQVDISNGLDWSLDHKIFYYIDSLSYSVDAFDY 180
                        ************************************************************

RGNWT1                  DLQTGQISNRRSVYKLEKEEQIPDGMCIDAEGKLWVACYNGGRVIRLDPVTGKRLQTVKL 187
HomosapiensNM_004683    DLQTGQISNRRSVYKLEKEEQIPDGMCIDAEGKLWVACYNGGRVIRLDPVTGKRLQTVKL 240
                        ************************************************************

RGNWT1                  PVDKTTSCCFGGKNYSEMYVTCARDGMDPEGLLRQPEAGGIFKITGLGVKGIAPYSYAG 246
HomosapiensNM_004683    PVDKTTSCCFGGKNYSEMYVTCARDGMDPEGLLRQPEAGGIFKITGLGVKGIAPYSYAG 299
                        ************************************************************



CLUSTAL 2.0.12 multiple sequence alignment


HomosapiensNM_004683    MSSIKIECVLPENCRCGESPVWEEVSNSLLFVDIPAKKVCRWDSFTKQVQRVTMDAPVSS 60
D4NheI4                 MSSIKIECVLPENCRCGESPVWEEVSNSLLFVDIPAKKVCRWDSFTKQVQRVTMDAPVSS 60
                        ************************************************************

HomosapiensNM_004683    VALRQSGGYVATIGTKFCALNWKEQSAVVLATVDNDKKNNRFNDGKVDPAGRYFAGTMAE 120
D4NheI4                 VALRQSGGYVATIGTKFCALNWKEQSAVVLATVDNDKKNNRFNDGKVDPAGRYFA----- 115
                        ********************************************************

HomosapiensNM_004683    ETAPAVLERHQGALYSLFPDHHVKKYFDQVDISNGLDWSLDHKIFYYIDSLSYSVDAFDY 180
D4NheI4                 ------------------------------------------------------------

HomosapiensNM_004683    DLQTGQISNRRSVYKLEKEEQIPDGMCIDAEGKLWVACYNGGRVIRLDPVTGKRLQTVKL 240
D4NheI4                 -------ANRRSVYKLEKEEQIPDGMCIDAEGKLWVACYNGGRVIRLDPVTGKRLQTVKL 168
                              **************************************************

HomosapiensNM_004683    PVDKTTSCCFGGKNYSEMYVTCARDGMDPEGLLRQPEAGGIFKITGLGVKGIAPYSYAG 299
D4NheI4                 PVDKTTSCCFGGKNYSEMYVTCARDGMDPEGLLRQPEAGGIFKITGLGVKGIAPYSYAG 227
                        ************************************************************CLUSTAL 2.0.12
```

multiple sequence alignment

```
HomosapiensNM_004683      MSSIKIECVLPENCRCGESPVWEEVSNSLLFVDIPAKKVCRWDSFTKQVQRVTMDAPVSS 60
D4-5NheI2                 MSSIKIECVLPENCRCGESPVWEEVSNSLLFVDIPAKKVCRWDSFTKQVQRVTMDAPVSS 60
                          ************************************************************

HomosapiensNM_004683      VALRQSGGYVATIGTKFCALNWKEQSAVVLATVDNDKKNNRFNDGKVDPAGRYFAGTMAE 120
D4-5NheI2                 VALRQSGGYVATIGTKFCALNWKEQSAVVLATVDNDKKNNRFNDGKVDPAGRYFAG---- 116
                          ********************************************************

HomosapiensNM_004683      ETAPAVLERHQGALYSLFPDHHVKKYFDQVDISNGLDWSLDHKIFYYIDSLSYSVDAFDY 180
D4-5NheI2                 ------------------------------------------------------------

HomosapiensNM_004683      DLQTGQISNRRSVYKLEKEEQIPDGMCIDAEGKLWVACYNGGRVIRLDPVTGKRLQTVKL 240
D4-5NheI2                 -----------------------------------------------------KRLQTVKL 124
                                                                                ********

HomosapiensNM_004683      PVDKTTSCCFGGKNYSEMYVTCARDGMDPEGLLRQPEAGGIFKITGLGVKGIAPYSYAG 299
D4-5NheI2                 PVDKTTSCCFGGKNYSEMYVTCARDGMDPEGLLRQPEAGGIFKITGLGVKGIAPYSYAG 183
                          ************************************************************
```